A dual role for DNA binding by Runt in activation and repression of *sloppy paired* transcription

Lisa Prazak[a,b,e,*], Yasuno Iwasaki[b], Ah-Ram Kim[c,†], Konstantin Kozlov[d], Kevin King[b,e,‡], and J. Peter Gergen[b]

[a]Department of Biology, Farmingdale State College, Farmingdale, NY 11735-1021, [b]Department of Biochemistry and Cell Biology and Center for Developmental Genetics, [c]Graduate Program in Biochemistry and Structural Biology, and [e]Graduate Program in Molecular and Cellular Biology, Stony Brook University, Stony Brook, NY 11794-5215; [d]Department of Applied Mathematics, St. Petersburg State Polytechnical University, St. Petersburg, Russia 195251

ABSTRACT **This work investigates the role of DNA binding by Runt in regulating the *sloppy paired 1* (*slp1*) gene and in particular two distinct *cis*-regulatory elements that mediate regulation by Runt and other pair-rule transcription factors during *Drosophila* segmentation. We find that a DNA-binding–defective form of Runt is ineffective at repressing both the distal (DESE) and proximal (PESE) early stripe elements of *slp1* and is also compromised for DESE-dependent activation. The function of Runt-binding sites in DESE is further investigated using site-specific transgenesis and quantitative imaging techniques. When DESE is tested as an autonomous enhancer, mutagenesis of the Runt sites results in a clear loss of Runt-dependent repression but has little to no effect on Runt-dependent activation. Notably, mutagenesis of these same sites in the context of a reporter gene construct that also contains the PESE enhancer results in a significant reduction of DESE-dependent activation as well as the loss of repression observed for the autonomous mutant DESE enhancer. These results provide strong evidence that DNA binding by Runt directly contributes to the regulatory interplay of interactions between these two enhancers in the early embryo.**

Monitoring Editor
Tom Misteli
National Institutes of Health, NCI

Received: Aug 5, 2020
Revised: Aug 13, 2021
Accepted: Aug 18, 2021

INTRODUCTION

The transcription factor encoded by the *Drosophila runt* gene provides a valuable model for investigating the regulation of gene expression by Runx proteins, a family of DNA-binding proteins that is conserved from basal metazoans, such as cnidarians and sponges, to humans (Sullivan *et al.*, 2008). Runx proteins participate in multiple pathways, extending from pattern formation and sex determination in *Drosophila* to the specification of cell fates in all three germ layers during mammalian development (Duffy and Gergen, 1994; Lian *et al.*, 2003; de Bruijn and Speck, 2004; Enomoto *et al.*, 2004; Ito, 2004). Aberrations in Runx activity are associated with a number of pathological conditions in humans. *Runx1*, also known as *AML1*, was initially identified as a frequent target of chromosome rearrangements involved in leukemia (Miyoshi *et al.*, 1993; Nucifora *et al.*, 1993; Golub *et al.*, 1995; Gamou *et al.*, 1998) and is now implicated in a variety of hematologic disorders (Yamagata *et al.*, 2005). Mutations in *Runx2* are associated with cleidocranial dysplasia (Mundlos *et al.*, 1997; Otto *et al.*, 1997), and alterations in Runx2 activity are associated with osteosarcoma as well as forms of breast, pancreatic, and prostate cancer (Kayed *et al.*, 2007; Pratap *et al.*, 2008; Akech *et al.*, 2010). Similarly, *Runx3* has roles in melanoma, breast, and colon cancer (Goel *et al.*, 2004; Lau *et al.*, 2006; Kitago *et al.*, 2009; Zhang *et al.*, 2011; Shin *et al.*, 2018) and has been identified as a susceptibility locus for ulcerative colitis (Weersma *et al.*, 2008). The finding that polymorphisms in Runx-binding sites are associated with a range of autoimmune diseases in humans (Prokunina *et al.*, 2002; Helms *et al.*, 2003; Tokuhiro *et al.*, 2003) further underscores the potential wide-ranging importance of this transcription factor family.

The hallmark of the Runx family is the Runt domain, a highly conserved 128-amino-acid domain that is responsible for DNA binding

This article was published online ahead of print in MBoC in Press (http://www.molbiolcell.org/cgi/doi/10.1091/mbc.E20-08-0509) on August 25, 2021.

‡Deceased.

†Present address: School of Life Science, Handong Global University, Pohang 37554, South Korea.

*Address correspondence to: Lisa Prazak (prazakl@farmingdale.edu).

Abbreviations used: ChIP, chromatin immunoprecipitation; Eve, even-skipped; Ftz, *fushi-tarazu*; *NGT*, *nanos-GAL4-tubulin*; Opa, odd-paired; *slp1*, *sloppy paired 1*.

and for interacting with the conserved CBFb/Bro partner proteins (Kagoshima *et al.*, 1993; Tang *et al.*, 2000; Bravo *et al.*, 2001; Zhang *et al.*, 2003). A mutant Runt protein that cannot bind to Bro partner proteins is defective in a number of different in vivo assays (Li and Gergen, 1999), strongly suggesting that all of Runt's regulatory activities involve this heteromeric transcription factor complex. In contrast, the DNA-binding activity of Runt does not appear to be required for the initial establishment of repression of the segment-polarity gene *engrailed* (Wheeler *et al.*, 2002; Vander Zwan *et al.*, 2003). This repression instead involves the Tramtrack transcription factor whose activity as a repressor is potentiated by Runt via an unknown mechanism. The DNA-binding–defective Runt[CK] protein retains certain activity, including the ability to disrupt anterior patterning in the embryo and to interfere with axonal targeting during eye development (Vander Zwan *et al.*, 2003; Walrad *et al.*, 2010). Runx proteins also regulate transcription via DNA-binding–independent pathways in mice (Wildey and Howe, 2009), indicating that this attribute is not unique to *Drosophila*. Indeed, the observation that factors such as the estrogen, glucocorticoid and PPARalpha nuclear receptors (Umayahara *et al.*, 1994; Porter *et al.*, 1997; Reichardt *et al.*, 1998; Tuckermann *et al.*, 1999; Delerive *et al.*, 2002; Cheung *et al.*, 2005) and the bHLH proteins Scl/Tal1 and Hand2 (Ravet *et al.*, 2004; Liu *et al.*, 2009), as well as members of the STAT transcription factor family (Cao *et al.*, 2011), all have regulatory functions that are DNA binding independent reinforces the need to validate the in vivo role of interactions between transcription factors and their specific *cis*-regulatory DNA targets.

Runt was initially characterized based on its vital role as a pair-rule gene in the *Drosophila* segmentation pathway (Nusslein-Volhard and Wieschaus, 1980; Gergen and Wieschaus, 1985, 1986). The extensive understanding of segmentation coupled with the tools available in the *Drosophila* system provides numerous advantages for investigating Runt function. The *slp1* gene has been identified as a particularly useful model. Runt functions both as an activator and as a repressor of *slp1* (Swantek and Gergen, 2004). The combinatorial rules that account for these dual regulatory properties were investigated using classical loss-of-function experiments in combination with an ectopic expression system that allows for quantitative manipulation of gene expression in the blastoderm embryo (Tracey *et al.*, 2000). Important to this regulatory dissection was the sensitivity of *slp1* to ectopic Runt and the finding that reproducible metameric changes in *slp1* expression are obtained with ectopic Runt at levels that do not significantly alter the metameric expression of other pair-rule genes that are involved in *slp1* regulation (Swantek and Gergen, 2004). Although this observation does not demonstrate that Runt directly regulates *slp1*, it strongly suggests that the initial response of *slp1* to ectopic Runt is not mediated through other known pair-rule gene regulators.

The initial metameric *slp1* pattern is composed of 14 two-cell-wide stripes in the posterior half of each parasegment (Figure 1A). This pattern of alternating stripes of *slp1*-expressing and nonexpressing cells can be divided into four different cellular contexts that repeat throughout the segmented region of the embryo, depending on the specific regulatory factors present in these cells (Figure 1A). Repression of *slp1* in type I cells is due to the homeodomain transcription factor Even-skipped (Eve) (Swantek and Gergen, 2004). Expression in type II cells, comprising the odd-numbered *slp1* stripes, is activated in response to Runt and Odd-paired (Opa), a Zn-finger transcription factor homologous to the mammalian Zic proteins (Mizugishi *et al.*, 2001). Type III cells also express Runt and Opa, but the presence of the homeodomain transcription factor encoded by the *fushi tarazu* (*ftz*) gene in these cells converts Runt from an activator to a repressor of *slp1* (Figure 1A). Finally, expression of *slp1* in type IV cells, comprising the even-numbered *slp1* stripes, is due to Opa plus a contribution from an unknown factor X.

Further insights on the regulation of *slp1* by Runt and the other pair-rule transcription factors came from the characterization of two distinct *cis*-regulatory elements that mediate this regulation (Prazak *et al.*, 2010). A proximal early stripe element (PESE) drives expression in type IV cells but fails to generate the Runt-dependent stripes in type II cells (Figure 1B). This enhancer mediates repression by Eve and by the combination of Runt and Ftz (Prazak *et al.*, 2010; Hang and Gergen, 2017), which can account for the lack of expression in cell types I, II, and III. The distal early stripe element (DESE) drives strong expression in type II and IV cells and also gives lower levels of inappropriate expression in type I cells. Consistent with this observation, this enhancer mediates repression by the combination of Runt and Ftz but is insensitive to repression by Eve (Prazak *et al.*, 2010). Important to this work, DESE has been demonstrated to mediate activation in response to Runt and Opa (Prazak *et al.*, 2010; Hang and Gergen, 2017). Interestingly, a composite reporter containing both early stripe elements recapitulates pair-rule gene–dependent regulation in a manner beyond what is expected from the additive inputs of the two separate enhancer elements. Recent studies on the mechanisms by which the activity of these enhancers is regulated have led to a proposal that this nonadditive interaction can be accounted for by enhancer-specific differences in the mode of repression in different cell types (Hang and Gergen, 2017).

Although several of the key factors involved in the differential regulation of *slp1* in these four different cell contexts are well defined, it remains to be established whether the Runt-dependent regulation of these enhancers is direct. Indeed, it has been suggested that Runt's role in this process is indirect (Clark and Akam, 2016). Previous work utilizing a temperature-sensitive allele of Runt provides evidence that there is a temporally acute role for Runt in *slp1* regulation, consistent with a direct interaction, but does not rule out an indirect role possibly through protein–protein interactions with other factors that directly interact with the *slp1* enhancers. Establishing whether the *slp1* PESE and DESE enhancers are direct targets of Runt is critical for understanding the mechanisms that underlie the nonadditive interactions between these two *cis*-regulatory elements. Here we investigate the role of DNA binding in the Runt-dependent regulation of these two early stripe enhancers. The DNA-binding activity of Runt is required for both activation and repression of *slp1* (Walrad *et al.*, 2010). As observed for endogenous *slp1*, the DNA-binding–defective Runt[CK] protein is ineffective at repressing the separate DESE and PESE enhancers as well as a composite reporter gene construct that contains both enhancers. Similarly, Runt[CK] is also compromised for activation of the composite reporter and the DESE enhancer, indicating that DNA binding by Runt contributes to Opa-dependent transcriptional activation. We further explore the function of presumptive Runt-binding sites in the DESE enhancer using site-specific transgenesis and quantitative imaging techniques. The results indicate that these sites are critical in mediating Runt-dependent repression in cell type III but are less important for activation in cell type II when DESE activity is examined as an autonomous enhancer. However, mutagenesis of these same sites in the context of a composite reporter that also contains PESE results in reduced expression in cell type II in addition to affecting repression in cell type III. We consider the implications of these findings for understanding *slp1* regulation in the context of models involving the competitive regulation of enhancer-promoter interactions by Runt and the pair-rule transcription factors and

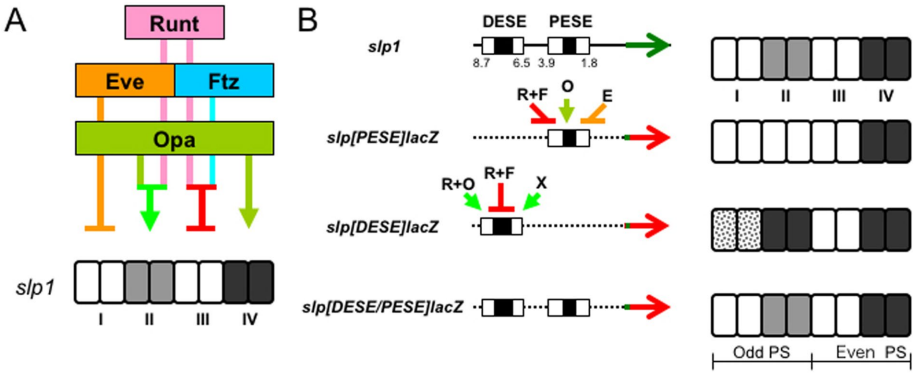

FIGURE 1: Regulation of *slp1* early stripe expression. (A) Schematic diagram of pair-rule regulatory inputs that generate the initial periodic expression of *slp1*. The phasing of the expression patterns of Runt, Eve, Ftz, and Opa are shown above a row of eight cells, representing two parasegmental repeats along the anterior–posterior axis. Shading indicates expression of *slp1* in type II and type IV cells, with darker shading indicating the stronger early expression in type IV cells. The green arrow above type II cells indicates the requirement for both Runt and Opa in their activation (Swantek and Gergen, 2004). The contribution of Opa to expression in type IV cells is similarly indicated by the arrow above these cells. Repression of *slp1* by Eve in type I cells is indicated by the orange horizontal bar and vertical line that connect to the domain of Eve expression indicated above these cells. The horizontal red bar above the *slp1*-repressed type III cells is connected to pink and blue vertical lines denoting the combined requirement for Runt and Ftz, respectively, in blocking expression (Swantek and Gergen, 2004). (B) The expression driven by *slp1* and different *slp-lacZ* reporters within a region spanning two parasegments is diagramed to the right as in A. A schematic of the *slp1* locus indicating the relative position of the upstream DESE and PESE enhancers relative to the transcription unit (green arrow) is provided at the top. The black boxes identify the minimal regions for each early stripe enhancer, from 8.1 to 7.1 kb and from 3.1 to 2.5 kb upstream of the transcription start site for the DESE and PESE enhancers, respectively (Prazak *et al.*, 2010). The white boxes identify the extent of DNA flanking the minimal enhancer segments contained in the composite reporter gene constructs used in this work to buffer potential short-range interactions between factors interacting with the different enhancer elements. These larger DNA segments extend from 8.7 to 6.5 kb and from 3.9 to 1.8 kb upstream of the transcription start site for DESE and PESE, respectively. The three lines below show schematics of the PESE-, DESE-, and [DESE + PESE]-containing *lacZ* (red arrow) reporter genes, with regions that are not contained in the reporters indicated by dotted lines. The pair-rule inputs mediated by the independent PESE and DESE enhancers are indicated above these elements (Prazak *et al.*, 2010), with the resulting expression diagramed to the right of each construct. The inappropriate expression in type I cells and stronger than normal expression in type II cells driven by the DESE enhancer are indicated by stippled and darkly shaded cells, respectively. DESE receives input from an unknown factor X that produces the residual expression in type IV cells in the absence of Opa. As shown at the bottom, the inappropriate activity of DESE is suppressed in a composite PESE-containing reporter that faithfully emulates the periodic expression of endogenous *slp1*.

discuss the potential importance of similar nonautonomous enhancer interactions in regulating gene expression in developmental systems.

RESULTS

Differential requirements for DNA binding in repressing the *slp1* early stripe enhancers

The role of DNA binding in the regulatory activities of Runt has previously been investigated using a mutant derivative containing two point mutations in the Runt domain (C127S, K199A) that greatly reduce in vitro DNA-binding activity. This DNA-binding–defective Runt[CK] protein retains the ability to establish repression of *engrailed* but is ineffective in activation of *Sex-lethal* as well as in both activation and repression of *slp1* (Kramer *et al.*, 1999; Vander Zwan *et al.*, 2003; Walrad *et al.*, 2010). To further clarify the requirement for DNA binding in *slp1* regulation, we used in situ hybridization to compare the activities of the Runt and Runt[CK] proteins on reporter gene constructs containing different *slp1 cis*-regulatory elements. Coexpression of Runt and Ftz using the *nanos-GAL4-tubulin* (*NGT*) maternal GAL4 expression system (Tracey *et al.*, 2000) resulted in the nearly complete repression of *slp1*. In the context of the cell-type nomenclature used here, ectopic coexpression of Runt and Ftz represses *slp1* in cell types II and IV and is driving all cells toward adopting the *slp1* expression state characteristic of cell type III. This nearly complete repression was faithfully emulated by the *slp[8765/3918]lacZ*^{P} reporter, a composite P-element reporter gene construct containing both the DESE and PESE pair-rule response elements (Figure 2, A and A′ and B and B′). Indeed, the merged image demonstrates good concordance in the irregular expression of the *slp1* and *lacZ* mRNAs that remains within the segmented region of the *slp1*-repressed embryos (Figure 2B″). In contrast, *NGT*-driven coexpression of Ftz and Runt[CK] had little effect on the expression of the even-numbered stripes in type IV cells of both *slp1* and the composite *slp[8765/3918]lacZ*^{P} reporter (Figure 2, C and C′). The reduced expression of the odd-numbered stripes in type II cells observed in these embryos was expected and is due to the ectopic expression of Ftz in type II cells that normally express endogenous Runt but not endogenous Ftz.

Similar experiments were performed to investigate the importance of DNA binding for Runt-dependent repression of reporter genes that contain only the PESE or DESE enhancers and are integrated into the same chromosome site using ΦC31 transgenesis. The PESE-containing *slp[3918]lacZ*^{att} reporter normally expresses only in type IV cells (Figure 2D). This expression was almost completely eliminated by *NGT*-driven coexpression of Runt and Ftz (Figure 2E). It is notable that the residual expression of this PESE-containing reporter does not overlap that of endogenous *slp1*. This discrepancy suggests that the integration of regulatory inputs by PESE does not contribute in a major way to the *slp1* pattern in these embryos. More important to the issue of whether DNA binding is important for the Runt-dependent repression of PESE is the observation that the expression of this reporter in type IV cells appears to be insensitive to ectopic coexpression of Runt[CK] and Ftz (Figure 2F). Indeed, the *lacZ* (magenta) expression driven by this PESE reporter gene appears to be broadened anteriorly, suggesting that the Runt[CK] protein interferes with repression of the reporter by endogenous Runt and Ftz in type III cells. Taken altogether, these results provide strong evidence that the DNA-binding activity of Runt is important for repression of the *slp1* PESE enhancer.

The response of the DESE-containing *slp[8771]lacZ*^{att} reporter is more complicated. This reporter faithfully emulates the response of the endogenous *slp1* gene to ectopic coexpression of wild-type Runt and Ftz (Figure 2H). This concordance is in contrast to the nonoverlapping expression of *slp1* and the PESE-containing *slp[3918]*

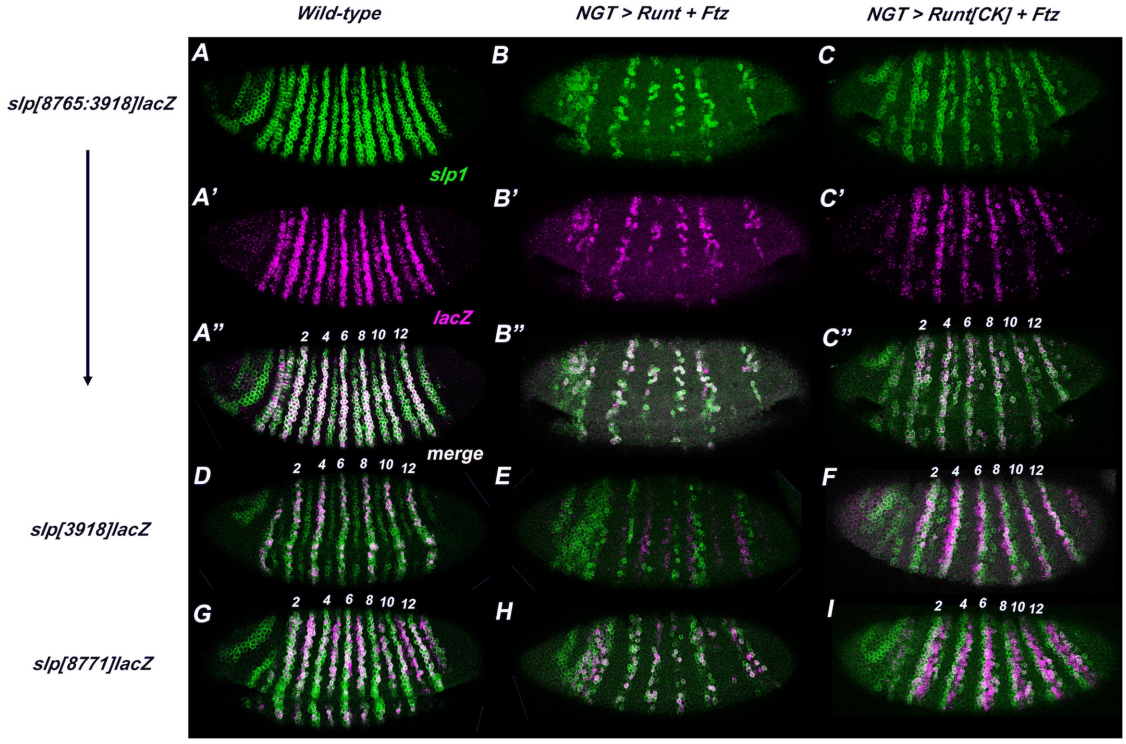

FIGURE 2: DNA binding by Runt is required for *slp1* repression. Fluorescence in situ hybridization of a gastrula stage wild-type embryo with the composite *slp[8765:3918]lacZ*^{P} reporter gene showing expression of *slp1* (A, green), *lacZ* (A′, magenta), and the merged image (A″). Note that the *slp1* mRNA is predominantly localized in the cytoplasm, whereas the *lacZ* mRNA expressed by the reporter genes used in this work has significant nuclear accumulation. Cells expressing both mRNAs appear as circles of magenta surrounded by white or at lower levels of *lacZ* expression green rings. This embryo in standard orientation has anterior to the left and dorsal side up. The composite reporter gene in this embryo contains both the DESE and PESE enhancers and in wild-type embryos mimics the early striped expression of *slp1*, including stronger even-numbered stripes, but is not expressed in the anterior head region. The response of *slp1* and this composite reporter gene to *NGT*-driven coexpression of Runt and Ftz or Runt[CK] and Ftz is shown with the same organization in B and C, respectively. The similarity in the response of *slp1* and the composite reporter to *NGT*-driven Runt and Ftz is most clearly demonstrated by the merged image (B″). Similarly, C″ shows resistance of the even-numbered stripes (labeled above embryo) of both *slp1* and the *lacZ* reporter to repression by Runt[CK] and Ftz. Merged fluorescence in situ hybridization images show the differential activities of the PESE-containing *slp[3918]lacZ*^{att} (D–F) and DESE-containing *slp[8771]lacZ*^{att} (G–I) reporters in these different genotypes. As previously described for wild-type embryos (Prazak *et al.*, 2010), PESE drives expression that coincides with the more strongly expressed even-numbered *slp1* stripes (D). This PESE-dependent expression is nearly fully repressed in response to Runt and Ftz (E), and the residual expressions of *lacZ* (magenta) and *slp1* (green) do not overlap. Coexpression of Runt[CK] and Ftz does not repress the overlapping even-numbered stripes of *slp1* and the *slp[3918]lacZ*^{att} reporter (F). For the DESE-containing reporter, the merged image of a wild-type embryo shows odd- and even-numbered *lacZ* stripes of similar intensities (G). The inappropriate activity of DESE in type I cells anterior to the odd stripes is close to the limits of detection with the nonsaturating settings used to capture these images but is reflected by intermittent magenta cells posterior to the even-numbered stripes. DESE-dependent expression is repressed by coexpression of Runt and Ftz (H). However, in contrast to PESE, the residual DESE-driven *lacZ* expression overlaps that of *slp1*. Runt[CK] is less effective than Runt at repressing the *slp[8771]lacZ*^{att} reporter (I), although *lacZ* (magenta) expression appears reduced in the *slp1*-expressing cells corresponding to the even-numbered stripes. The embryos in this figure were obtained from crosses between females homozygous for the *NGT40* driver and the appropriate reporter gene to males homozygous for *UAS-ftz*^{263} and the appropriate *UAS-runt* transgene. The *UAS-runt*^{15} and *UAS-runt[CK]*^{43} transgenes used in these experiments are expressed at similar levels and have equivalent activities on DNA-binding–independent targets of Runt (Vander Zwan *et al.*, 2003).

lacZ^{att} reporter in response to ectopic Runt and Ftz noted above (Figure 2E) and supports the proposal that the DESE enhancer is responsible for the regulation of *slp1* transcription in Runt-expressing cells (Hang and Gergen, 2017). However, there are interesting differences in the response of *slp1* and the *slp[8771]lacZ*^{att} reporter to ectopic coexpression of Runt[CK] and Ftz. It is most straightforward to interpret whether the effects of ectopic Runt[CK] expression are due to the inability to interact with DNA in cells that do not express endogenous Runt, that is, in cell type IV normally comprising the even-numbered *slp1* stripes and the type I cells posterior to these stripes. As observed for endogenous *slp1* and the PESE-containing reporter, ectopic expression of Runt[CK] in type IV cells does not result in repression of the *slp[8771]lacZ*^{att} reporter (Figure 2I). Somewhat unexpected is the strong expression of this reporter in type I cells, that is, in cells posterior to the even-numbered *slp1* stripes (Figure 2I). Although further work is needed to explain the DESE-dependent expression in type I cells in response to ectopic coexpression of Runt[CK] and Ftz, these results provide strong

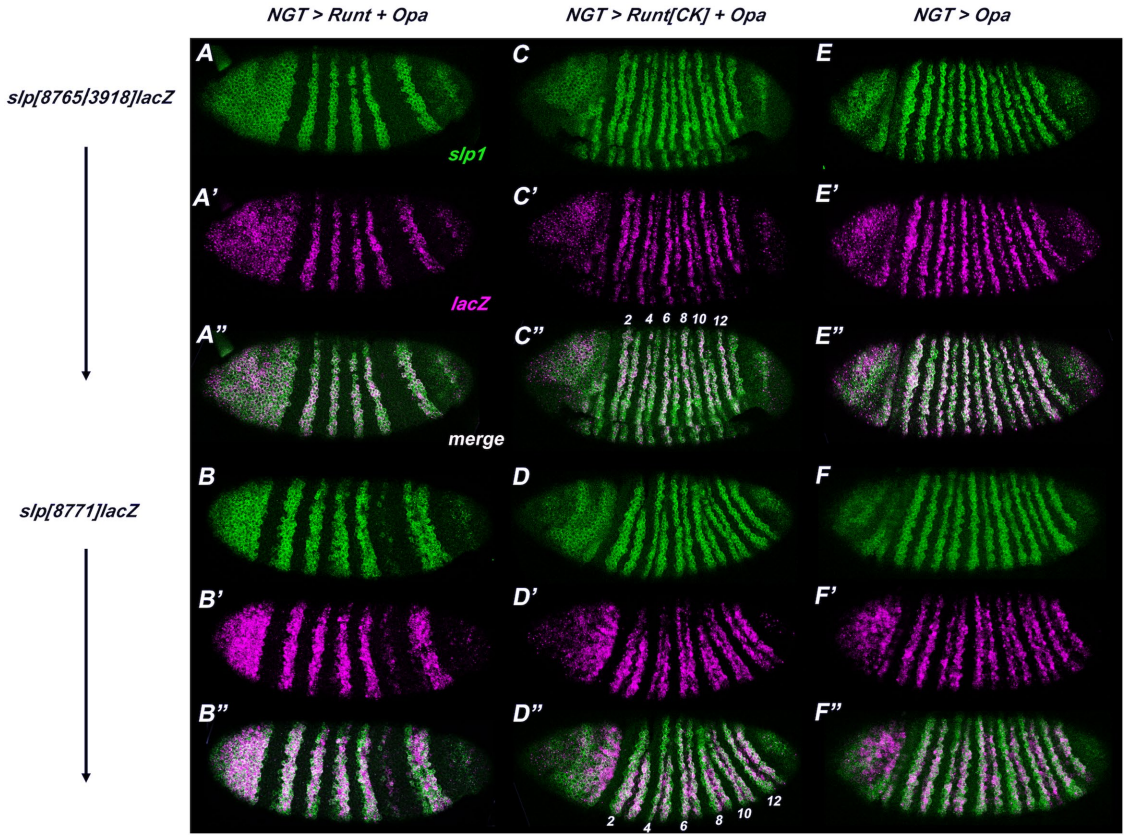

FIGURE 3: DNA-binding activity of Runt contributes to *slp1* activation. Fluorescence in situ hybridization showing expression of *slp1* (green) and *lacZ* (magenta) in embryos with *NGT*-driven coexpression of Opa with wild-type Runt (A, B) or Runt[CK] (C, D), as well as with *NGT*-driven Opa alone (E, F). As indicated on the left margin, embryos in A, C, and E have the composite *slp[8765:3918]lacZ*^{P} reporter, whereas embryos in B, D, and F have the DESE-containing *slp[8771]lacZ*^{att} reporter. Both the composite (A, A′) and DESE-only (B, B′) reporters mimic the strong anterior activation observed for *slp1* in response to ectopic Runt and Opa. The broad bands of cells that express neither *slp1* nor *lacZ* in these embryos are the result of repression by Runt and Ftz (Swantek and Gergen, 2004). Embryos with *NGT*-driven coexpression of Runt[CK] and Opa show some evidence of anterior activation of *slp1* and both the composite (C, C′) and DESE-containing (D, D′) reporters that is not observed in wild-type embryos (compare with Figure 2, A and A′), though at levels lower than produced by Runt and Opa. Expression of the DESE-containing *slp1[8771]lacZ*^{att} reporter is also increased in type I cells posterior to the even stripes (D″). A similar activation of DESE in these cells, as well as the partial anterior activation of *slp1* and both reporters in response to Runt[CK] and Opa, is obtained in response to *NGT*-driven expression of Opa alone (E, E′, F, F′). The embryos in these experiments were obtained from crosses between females homozygous for the *NGT40* driver and the appropriate reporter gene to males carrying the strong *UAS-opa*^{D10} transgene either alone or in combination with *UAS-runt*^{232} or *UAS-runt[CK]*^{77}, two transgenes that are expressed at similar levels and have equivalent activities on DNA-binding–independent targets of Runt (Vander Zwan *et al.*, 2003).

evidence that the DNA-binding activity of Runt is required for repression of both the PESE and DESE enhancers in type IV cells.

Runt's DNA-binding activity potentiates Opa-dependent *slp1* activation

We used an additional assay to further investigate the role of DNA binding by Runt in *slp1* activation. This assay takes advantage of the observation that coexpression of Runt and Opa results in *slp1* activation in all somatic cells of the blastoderm embryo that do not express Ftz (Swantek and Gergen, 2004), including cells in the anterior head region that are not expressing other pair-rule transcription factors (Figure 3A). The resulting pattern is nearly uniform anterior expression of *slp1* extending to cells at the anterior pole with five three- to four-cell-wide stripes of expression separated by four- to five-cell-wide bands of nonexpressing cells in the presegmental region of the embryo. The broader band of nonexpressing cells separating the fourth and fifth stripes is explained by the localized expression of Ftz throughout this region (Swantek and Gergen, 2004). The response of *slp1* to ectopic coexpression of Runt and Opa was faithfully emulated by a composite reporter gene containing both the DESE and PESE enhancers (Figure 3, A′ and A″) as well as by the DESE-containing *slp[8771]lacZ*^{att} reporter (Figure 3, B′ and B″). In contrast, the ectopic coexpression of Opa with Runt[CK] had much less of an effect on the metameric expression of *slp1* and the DESE-containing reporters (Figure 3, C′ and D′), suggesting that both activation and repression of these targets involves DNA binding by Runt. There is clear evidence for the ectopic expression of *slp1* and both DESE-containing reporters in anterior regions in Runt[CK]-expressing embryos versus wild-type embryos (compare Figure 3, C″ and D′ with Figure 2, A″ and G). This expression was more irregular and did not extend as far anteriorly, especially in ventral regions as observed in response to ectopic expression of

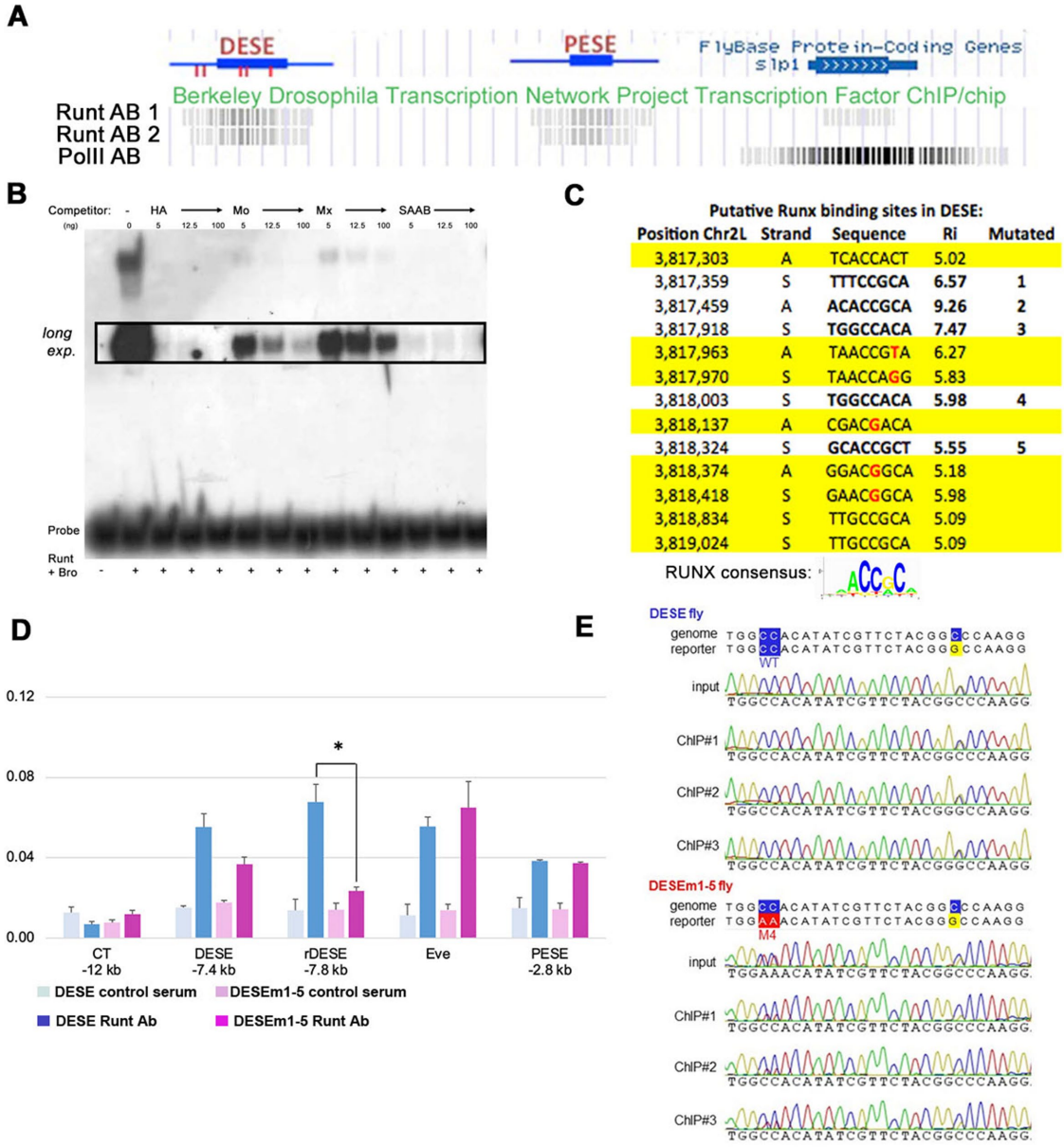

FIGURE 4: Identification of Runt-binding sites in the *slp1* DESE enhancer. (A) Genome Surveyor screen shot depicting results of genome-wide chromatin immunoprecipitation experiments for an approximately 10 kb interval flanking the *slp1* transcription unit performed with two different antisera directed against the Runt protein and one directed against the transcriptionally active phosphorylated form of RNA polymerase II on chromatin for stage 4–5 blastoderm embryos (MacArthur *et al.*, 2009). The extents of DNA sequences included in the *slp[DESE:8765]* and *slp[PESE:3918]* enhancers are indicated by blue lines above this screen shot, with the thicker regions corresponding to the central minimal elements (Prazak *et al.*, 2010). Data for all antibodies are shown with a threshold 1% false-discovery rate. (B) Results of electrophoretic mobility shift assays with recombinant Runt and Bro proteins and a labeled DNA probe containing the Runx site in the A core of the polyoma virus enhancer (Kamachi *et al.*, 1990). The two leftmost lanes show the fast-migrating probe alone and the additional more slowly migrating complex detected with Runt and Bro near the top of the autoradiogram, respectively. The inset in the black box shows a longer exposure of the region with Runt:Bro:DNA complexes. The other lanes show competition experiments with 5, 12.5, and 100 ng of four different oligonucleotide probes as labeled across the top. These probes contain Runx sites of different affinities. Their effectiveness as competitors correlates with their rank order of affinity for Runx1, HA ($K_d = 2.6 \times 10^{-12}$ M) > SAAB (5.5×10^{-12} M) > Mo (2.9×10^{-11} M) > Mx (1.7×10^{-10} M) (Lewis *et al.*, 1999). Comparable results were obtained in competition experiments done with oligonucleotide probes containing Runx sites from the SL3-3, TCRa, and SFFV (Rauscher) enhancers (unpublished data). (C) The sequence coordinates, orientation (Sense, Antisense), sequence, and Ri score based on a position weight matrix for a consensus Runx site are shown for candidate Runt sites in the region of the DESE enhancer. Nucleotides in a red font indicate base substitutions of one of the core cytosines in candidate sites with an Ri score greater than 5.1. The five sites with the highest Ri scores that also retain the core cytosines are numbered 1–5 on the right side of the table. The positions of these sites are indicated by red vertical lines below the schematic depiction of DESE in A. (D) Results of ChIP assays with control serum (light blue and light pink bars) and antibodies specific for Runt

Runt and Opa (Figure 3, A″ and B″). A similar level of anterior activation was produced in response to *NGT*-driven expression of Opa alone (Figure 3, E″ and F′). These observations indicate that ectopic expression of Opa alone can activate *slp1* and the DESE-containing reporter gene constructs in the absence of Runt and suggests that this Opa-dependent transcription is potentiated by Runt in a DNA-binding–dependent manner.

Runt-binding sites mediate repression by the *slp1* DESE enhancer

The results of the above experiments provide evidence that the DNA-binding activity of Runt contributes to both the activation and repression of the *slp1* early stripe enhancers but do not demonstrate that this involves direct interactions between Runt and the *slp1* enhancers. The sensitivity of *slp1* expression to manipulations in Runt activity, as well as the temporal immediacy of the response to these manipulations (Swantek and Gergen, 2004), are consistent with *slp1* being a direct target. Further, results from the Berkeley Drosophila Transcription Network Project (BDTNP) identify regions of the *slp1* locus that are associated with Runt in the early *Drosophila* embryo (MacArthur *et al.*, 2009). The two regions that show the highest levels of association with both Runt antisera used in these studies correspond remarkably well with the DESE and PESE enhancers identified by our functional studies on *slp1* regulation (Figure 4A). Several studies have identified the sequence ACCRCA as a consensus Runx-binding site (Kamachi *et al.*, 1990; Melnikova *et al.*, 1993). The structure of Runx1 bound to DNA has been determined (Bravo *et al.*, 2001; Tahirov *et al.*, 2001). The six amino acids that are the primary determinants of Runx1 DNA-binding specificity are all identical in *Drosophila* Runt, strongly suggesting that binding sites recognized by Runt will conform to the Runx consensus. The similar DNA-binding specificity of Runt was confirmed by electrophoretic mobility shift assays using a series of oligonucleotide competitors that have different affinities for mammalian Runx1 (Lewis *et al.*, 1999). The results of these experiments revealed that Runt has the same rank order of affinities for these different sequences (Figure 4B). On the basis of these observations, we used a Runx position weight matrix to identify putative Runt-binding sites in DESE as a starting point for investigating whether direct interactions with the DESE enhancer are involved in the regulation of DESE-dependent transcription by Runt. This search identified a number of candidate sites of varying quality within the interval defined by the DESE-containing *slp[8771]lacZ*^{att} reporter gene (Figure 4C). Of these sites, five were chosen for mutagenesis based on having a high Ri value as well as containing the core cytosines in the consensus sequence that contribute most to DNA-binding specificity.

We used chromatin immunoprecipitation (ChIP) to investigate whether mutagenesis of these five putative binding sites affected the association of Runt with the DESE enhancer. ChIP assays were performed on chromatin from 3- to 4-h-old *Drosophila* embryos containing either the wild-type *slp[8771]lacZ*^{att} or the mutant *slp[8771m1-5]lacZ*^{att} reporter with mutations in all five of the candidate Runt sites. Results of quantitative PCR with the rDESE-7.8 primer pair that takes advantage of a sequence polymorphism to specifically amplify the region containing Runt sites 3 and 4 from the DESE-containing reporter genes revealed that the ChIP signal observed with the wild-type DESE-containing reporter is significantly reduced ($p < 0.05$) near to background levels for the reporter with the mutant Runt-binding sites (Figure 4D). The effect of these mutations on Runt association is further confirmed by direct sequencing of the PCR products obtained using primers that amplify a region containing Runt candidate binding site 4 for both endogenous *slp1* and these reporter genes. The sequence chromatogram of the PCR product obtained with input chromatin from *slp[8771m1-5]lacZ*^{att} embryos shows both the wild-type GCCACA sequence from the endogenous *slp1* locus and the GAAACA sequence for the mutant binding site in the reporter gene (Figure 4E). In contrast, the sequence of the PCR product from the ChIP assay with this mutant reporter gene shows a loss of adenine base calls from the mutant Runt-binding site (Figure 4E). These results confirm the in vivo association of Runt with the DESE-containing *slp[8771]lacZ*^{att} reporter gene and provide strong evidence that mutation of the Runt sites within this element interfere with this interaction.

We used ΦC31-mediated site-specific transgenesis to investigate the effects of mutations in these five candidate Runt-binding sites, both singly and in a number of different combinations. None of the single site mutants that were tested showed obvious effects on reporter gene expression (Supplemental Figure 1). The region within DESE that showed the highest level of Runt association in the BDTNP results encompasses Runt sites 3 and 4 (Figure 4A). A *DESE-lacZ* reporter gene containing mutations in both of these sites, *slp[8771m3,4]lacZ*^{att} produced an altered pattern. Expression of both the odd- and even-numbered stripes persisted, but with a clear loss of repression in the type III cells anterior to stripes 8, 10, and 12 (Figure 5, B′ and B″). The loss of repression is more apparent for a reporter containing mutations in all five of the candidate Runt

(dark blue and magenta bars) using chromatin from embryos homozygous for either the wild-type *slp[8771]lacZatt* (DESE) or *slp[8771m1-5]lacZatt* (DESEm1-5) reporter genes. The CT primer pair amplifies a region 12 kb upstream of the *slp1* transcription start site as a negative control for Runt association. Primer pair DESE –7.4 kb amplifies a region of DESE containing Runt site 5 for both endogenous *slp1* and the DESE-containing reporter genes. Primer pair rDESE –7.8 kb takes advantage of a polymorphism to specifically amplify a region of the DESE-containing reporter genes containing Runt sites 3 and 4. The Eve primer pair amplifies a region of the *eve* minimal autoregulatory sequence (MAS) that has strong association with Runt (MacArthur *et al.*, 2009) as a positive control. Primer pair PESE –2.8 kb amplifies a region of the endogenous *slp1* PESE enhancer that provides a second positive control for the efficiency and sensitivity of these ChIP assays in detecting Runt binding with chromatin from embryos containing the wild-type DESE and DESEm1-5 reporter genes. The asterisk above the bar between the wild-type DESE and DESEm1-5 reporter genes for the rDESE –7.8 kb primer pair indicates a statistically significant (p value < 0.05) reduction in the association of Runt with the DESEm1-5 reporter. Although the difference is not statistically significant, the reduced ChIP signal for the DESE –7.4 kb primer pair is expected based on the reduced association of Runt with the DESEm1-5 reporter but not with the endogenous *slp1* DESE enhancer. (E) Chromatograms of sequence results from input DNA as well as three independent Runt ChIP assays for either the wild-type DESE or DESEm1-5 enhancer using primers that amplify a region of DESE containing Runt site 4 for both the endogenous and reporter DESE sequences. Shaded boxes indicate the two C > A mutations that were introduced to mutate Runt site 4 as well as the C > G sequence polymorphism that distinguishes the DESE-containing reporters from the endogenous *slp1* locus.

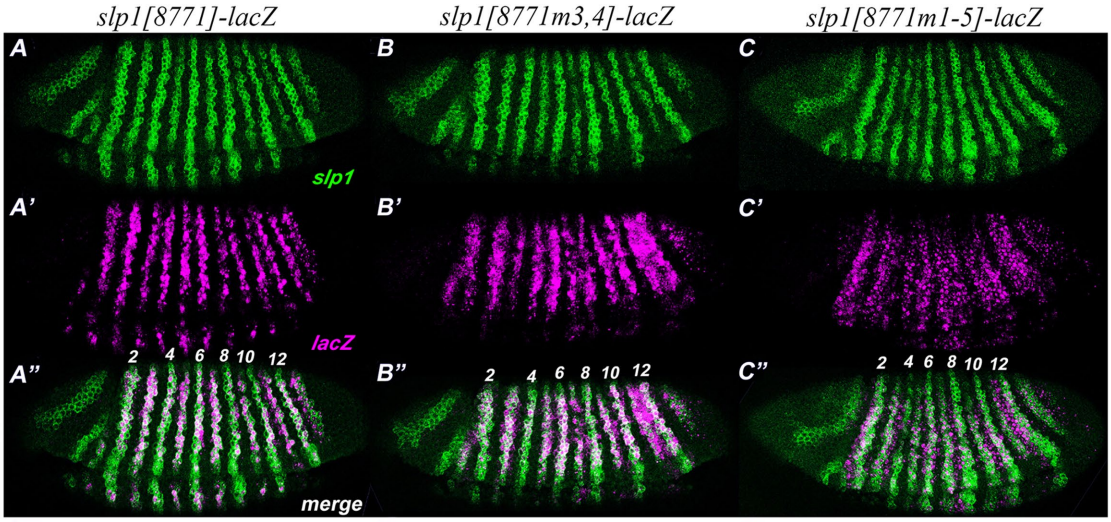

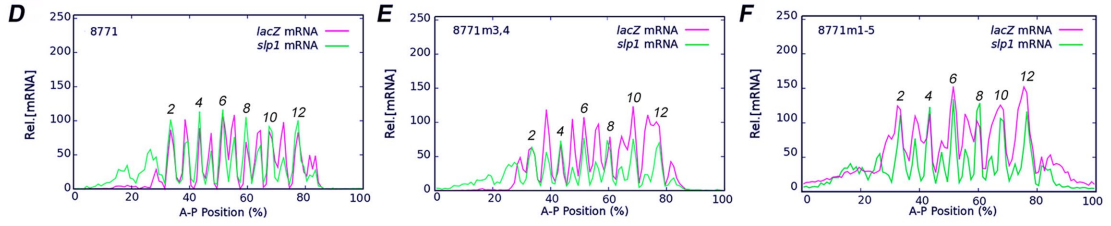

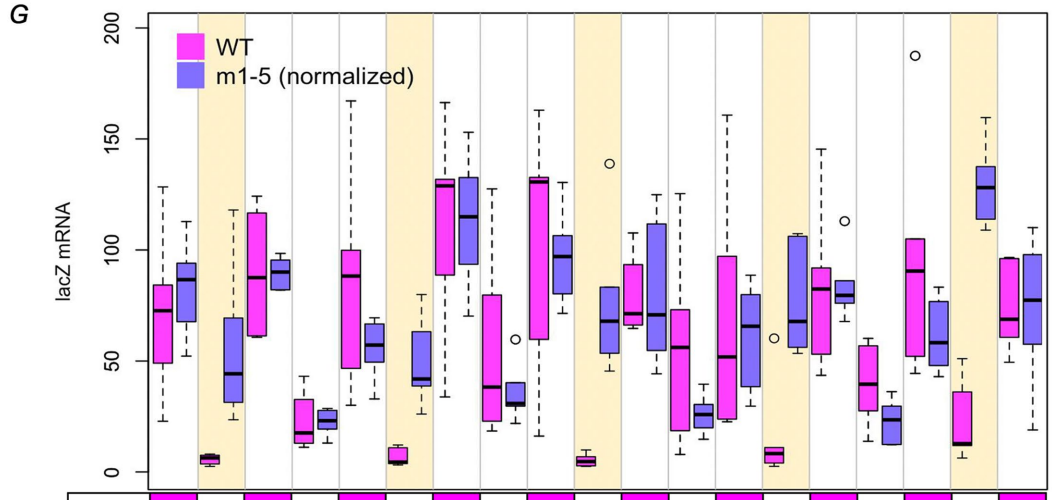

Stripe	3		4		5		6		7		8		9		10		11		12
Cell type	II	III	IV	I	II	III	IV	I	II	III	IV	I	II	III	IV	I	II	III	IV
WT	71.6	5.72	89.6	22.5	86.7	6.48	113	54.1	105.4	5.23	79	56.1	67.9	15.7	83.1	39.5	94.9	21.8	73.4
MT	105.4	69.7	113.5	28.4	72	63.1	147	46.1	119.8	94	98.1	32.1	97.3	121.3	132.7	36.3	69.6	147	83.1
nMT	83.3	55.1	89.7	22.5	55.4	48.7	113.2	35.6	97.1	76.1	79.5	26.1	61.3	76.5	83.7	22.9	61.2	129.4	73.2
nMT/WT	1.16	9.67	1	1	0.64	7.49	1	0.66	0.92	14.63	1.01	0.46	0.9	4.87	1.01	0.58	0.64	5.94	1
p-value	0.5	0.01	0.99	0.99	0.17	0.002	0.99	0.33	0.74	0.003	0.97	0.14	0.79	0.001	0.97	0.08	0.17	1.2e-6	0.99

FIGURE 5: Runt sites mediate repression of DESE-driven expression. Fluorescence in situ hybridization shows expression of *slp1* (green) and *lacZ* (magenta) for reporter gene constructs containing the wild-type *slp[8771]*lacZ^{att} reporter (A) compared with similar reporter gene constructs inserted at the identical genomic location that have mutations in Runt sites 3 and 4 (B) or in all five putative Runt-binding sites (C). The even-numbered stripes are labeled above the merged images for these three embryos shown in panels A″, B″, and C″, respectively. (D–F) Integrated expression patterns of these reporter gene constructs generated using an image processing method that allows averaging of results from multiple embryos (Janssens *et al.*, 2005) that has been extended to include *slp1* expression in stage 6 embryos as described in *Materials and Methods*. Relative mRNA accumulation levels are plotted as a function of position on the A–P axis, with *slp1* and *lacZ* indicated by the green and magenta traces, respectively. As above, the even-numbered *slp1* stripes are labeled to provide reference points for the descriptions provided in the text. It is notable that the trace of *slp1* expression approaches background levels anterior to both the odd- and even-numbered

sites, *slp[8771m1-5]lacZ*^{att}. The effect of these mutations was a loss of repression in the type III cells anterior to all of the even-numbered stripes (Figure 5, C′ and C″). This derepression occurs in cells where repression normally requires both Runt and Ftz. On the basis of these observations, we conclude that the Runt-binding sites in DESE are important for its repression by Runt and Ftz. Expression of the mutant reporter was not uniform, with somewhat higher levels of expression in type III cells anterior to even-numbered *slp1* stripes than in the type I cells posterior to these stripes.

To validate the above observations and gain further insight into the possible effects of the Runt-binding site mutations on reporter gene expression, we used a process for quantifying confocal in situ hybridization data (see *Materials and Methods*). In this case data were collected and integrated for stage 6 *Drosophila* embryos, a brief (<10 min) stage with distinctive morphology during which the initial metameric *slp1* pattern is evident. The differences in expression of endogenous *slp1* and the DESE-containing *slp[8771]lacZ*^{att} reporter were confirmed by this analysis (Figure 5D; Supplemental Figure 2). The difference in expression levels in even-versus-odd stripes observed for the *slp1* mRNA (green trace) was much less apparent for *lacZ* (magenta trace). The inappropriate expression of this reporter gene in type I cells anterior to the odd stripes was also demonstrated by *lacZ* mRNA levels above background that are not observed for *slp1*, especially anterior to stripes 7 and 11 (i.e., posterior to stripes 6 and 10). A similar representation of the results for the reporter with mutations in Runt sites 3 and 4 confirmed the loss of repression in type III cells anterior to stripes 8, 10, and 12 and also provided an indication of partial loss of repression anterior to other even-numbered stripes (Figure 5E). Indeed, the *lacZ* mRNA levels due to loss of repression in type III cells anterior to the even stripes were consistently higher than in type I cells posterior to these stripes. The same pattern was observed for the quintuple mutant *slp[8771m1-5]lacZ*^{att} reporter (Figure 5F), with consistently higher levels of expression occurring in type III cells anterior to the even *slp1* stripes than in type I cells posterior to the even *slp1* stripes. Analysis of normalized expression data for the *slp[8771]lacZ*^{att} (WT) and slp[*8771m1-5]lacZ*^{att} (MT) reporters shows a statistically significant increase in *lacZ* expression in all five of the different type III cells in which expression was quantified (Figure 5G). These quantitative results provide strong evidence that the Runt-binding sites in DESE are important for the Runt-dependent repression of this enhancer in cell type III. Interestingly, this analysis revealed no discernible effect of the Runt-binding site mutations on DESE-driven activation in type II cells.

Runt binding also contributes to DESE-dependent activation

The DNA-binding activity of Runt contributes to *slp1* activation (Walrad *et al*., 2010), an effect that is emulated by a composite reporter gene containing both the PESE and DESE enhancers (Figure 3). We previously showed that Runt-dependent activation is mediated by DESE and not by PESE (Prazak *et al*., 2010). However, as shown above, mutagenesis of five candidate Runt-binding sites in DESE greatly interferes with repression in type III cells but does not significantly reduce the expression of the reporter gene in type II cells. One explanation for these somewhat paradoxical results is that the relative importance of Runt DNA binding for DESE-dependent activation is increased by the presence of the PESE enhancer. This could be due to Runt interacting with the DESE and/or PESE enhancers. To further investigate whether activation involves Runt binding to DESE we examined

stripes in all three graphs. In contrast, *slp[8771]lacZ*^{att} expression approaches background levels anterior to all of the even- but not the odd-numbered *slp1* stripes (D). The loss of repression of *slp[8771m3,4]lacZ*^{att} (E) and *slp[8771m1-5]lacZ*^{att} (F) in type III cells anterior to the even-numbered stripes is demonstrated by even stripes with shoulders of anterior expression at levels that are comparable to (if not greater than for the quintuple mutant) the levels measured in cells that express the odd-numbered *slp1* stripes. The integrated expression patterns presented in panels D, E, and F were generated by averaging registered quantitative data obtained from four, five, and five stage 6 embryos, respectively. See Supplemental Figure 2 for the raw data black-and-white images of *slp1* and *lacZ* in situ hybridization of stage 6 embryos used for quantifying these expression patterns. (G) Statistical analysis of normalized expression data for the *slp[8771]lacZ*^{att} (WT) and slp[*8771m1-5]lacZ*^{att} (MT) reporters is provided with boxplots showing the range of expression along with a table of the mean expression values (both raw data and normalized) in different cell types from *slp1* stripes 3–12 along the A–P axis. Data points that were excluded as outliers are indicated by circles. The magenta boxes numbered 3–12 at the top row of the table indicate the location of the *slp1* stripes in relation to the boxplots above. Row 2 of the table shows the four different cell types extending from the type II cells comprising *slp1* stripe 3 to the type IV cells comprising stripe 12. *LacZ* expression was measured at the peak of each stripe with the position (% egg length = EL) taken from the averaged *slp1* mRNA expression pattern as follows. Stripe 3 (S3) = 39; S4 = 43; S5 = 47; S6 = 51; S7 = 55; S8 = 59; S9 = 64; S10 = 67; S11 = 72; S12 = 77. Expression in the type I and III cells located between different *slp1* stripes was measured at an A–P position halfway between the peaks of the adjacent stripes, for example, the *lacZ* expression level reported for the type III cells between *slp1* stripes 3 and 4 was the level measured at 41% EL. The raw data for the averaged *lacZ* expression levels from WT and MT embryos are shown in table rows 3 and 4. Differences in the expression levels measured between the WT and MT embryos were normalized using the mean expression level in type IV cells as these cells have high levels of expression for *slp1* and both the WT and MT reporters. Normalized MT data are indicated as nMT on the left side of table row 5, with the normalized values in type IV cells indicated by the blue-shaded cells in table rows 3 (WT) and 5 (nMT). Expression values from type I and III cells were normalized using the expression level for the adjacent type IV cells. Expression values from type II cells were normalized using the values for the next most posterior type IV cell. Table row 6 shows the ratio of the average nMT to WT expression levels. The magenta and blue boxplots indicate the normalized expression levels measured in embryos containing the WT and MT reporters, respectively. The boxplots for expression in the type III cells anterior to the even-numbered *slp1* stripes (indicated by beige backgrounds) show consistently higher levels of nMT expression relative to WT. A Welch unpaired two-sample *t* test (two tailed) was conducted for each of the different cell types included in this figure. Significant *p* values (≤0.01) are highlighted in green (if $m_{WT} \neq m_{nMT}$, m: mean of a group). Note that only the five different type III cells included in this analysis (shaded in green) showed differences in *lacZ* expression that are statistically significant ($p \leq 0.01$).

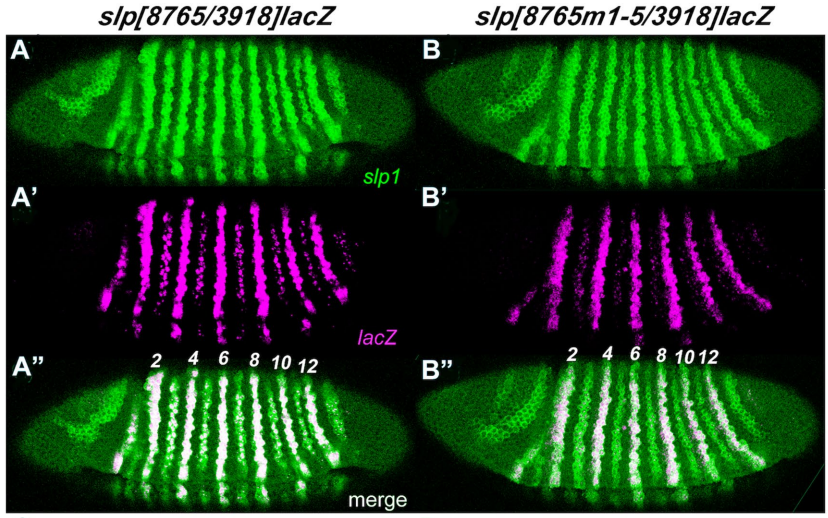

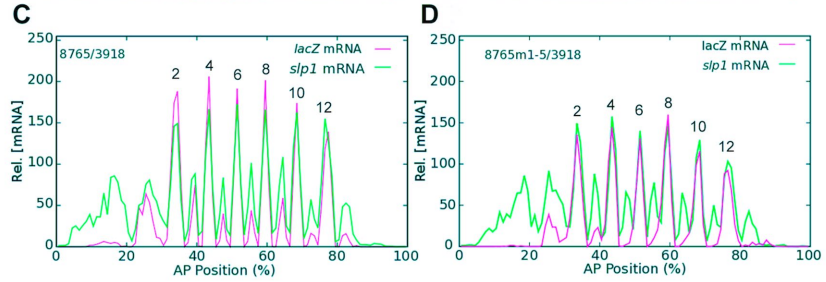

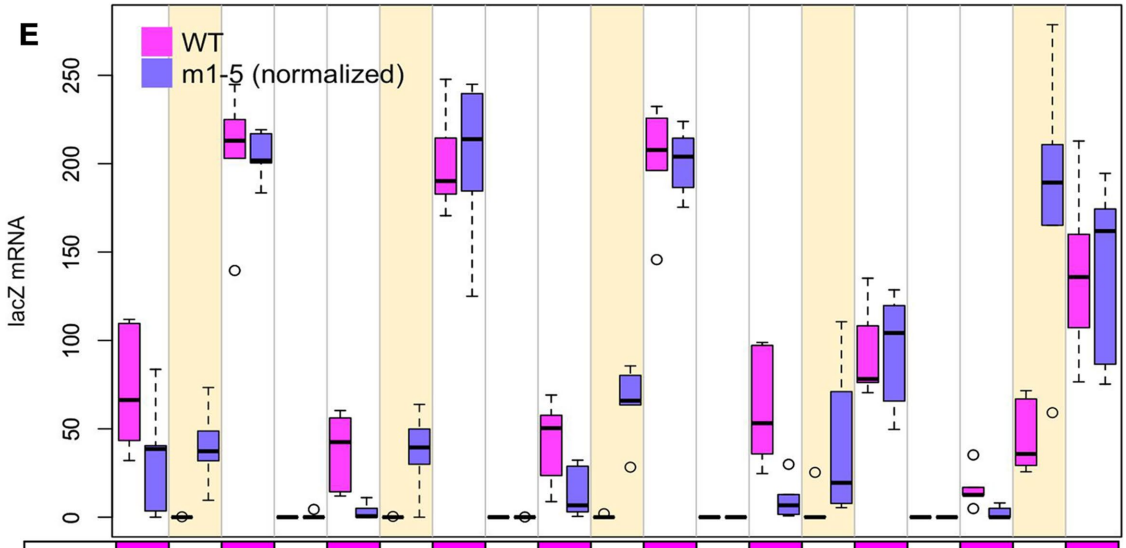

Stripe	3		4		5		6		7		8		9		10		11		12
Cell type	II	III	IV	I	II	III	IV	I	II	III	IV	I	II	III	IV	I	II	III	IV
WT	72.6	0.05	205	0	37	0.08	201.1	0	41.9	0.4	201.5	0	61.9	5.16	93.6	0	16.4	45.8	138.5
MT	23.2	28.07	142.9	0.62	2.15	23.5	129.2	0.01	11.2	50.9	158.1	0	10.9	45.1	98.5	0	1.37	94	72.14
nMT	33.26	40.18	204.38	0.89	3.34	36.63	201.58	0.03	14.27	64.72	200.84	0	10.37	42.86	93.59	0	2.61	180.6	138.51
nMT/WT	0.46	803	1	Inf	0.09	407.33	1	Inf	0.34	161.82	1	NaN	0.17	8.29	1	NaN	0.16	3.94	1
p-value	0.059	0.009	0.486	0.187	0.014	0.014	0.506	0.187	0.037	0.001	0.485	NaN	0.013	0.072	0.501	NaN	0.025	0.009	0.5

FIGURE 6: Runt-binding sites in DESE contribute to both activation and repression of the composite DESE + PESE reporter gene. (A) Expression of *slp1* (green), the wild-type composite *slp[8765/3918]lacZ*^{att} reporter (magenta, A′), and the merged image (A″) as visualized by fluorescence in situ hybridization. (B, B′, B″) Similar representation of the expression of the mutant *slp[8765m1-5/3918]lacZ* reporter inserted in the same genetic location and identical in sequence to the wild-type reporter in A except for the mutations in the five Runt-binding sites in the DESE enhancer. In addition to having reduced expression of the odd-numbered stripes, the mutant reporter also shows evidence of

the effect of mutating the Runt sites in DESE in the context of a composite reporter that also contains PESE. This experiment compares expression of wild-type and mutant composite reporter gene constructs integrated into the same genomic site using ΦC31 site-directed trangenesis. Similar to the composite *slp[8765/3918]lacZ*^{p} reporter described previously and used in Figures 2 and 3, the wild-type *slp[8765/3918]lacZ*^{att} transgene expressed both odd and even stripes, with weaker expression of the odd-numbered stripes as observed for endogenous *slp1* (Figure 6, A and A′). The composite construct with mutations in the five Runt sites, *slp[8765m1-5/3918]lacZ*^{att}, also gave strong expression of the even stripes, but with reduced expression of the odd-numbered stripes (Figure 6, B, B′, and B″; Supplemental Figure 3). Quantification of the wild-type and mutant composite reporter gene expression patterns confirmed these qualitative observations. The mutant reporter showed greatly reduced expression in *slp1*-expressing type II cells comprising the odd stripes, with the residual expression most obvious for stripe 3 (Figure 6D). Further, the symmetric stripes of *lacZ* mRNA accumulation observed for the wild-type composite reporter (Figure 6C) are replaced by even-numbered stripes that show an anterior shoulder of lower-level expression in the *slp[8765m1-5/3918]lacZ*^{att} embryos (Figure 6D). This derepression in type III cells is analogous to that observed for *slp[8771m1-5]lacZ*^{att}. Statistical analysis of normalized expression data for the *slp[8765/3918]lacZ* (WT) and *slp[8765m1-5/3918]lacZ* (MT) reporters reveals reduced expression in type II cells, with a ratio of nMT to WT expression between 0.09 and 0.46 (Figure 6E). This reduction is statistically significant ($p \leq 0.05$) for four of the five type II cells (shaded in yellow) included in this analysis. This analysis also indicates a statistically significant increase in expression in type III cells ($p \leq 0.01$, shaded in green). Taken altogether, these observations indicate that mutating the Runt sites in the DESE enhancer affects both the repression and activation mediated by this enhancer. Notably the importance of the Runt-binding sites for activation is significant only in the composite reporter gene construct containing the PESE enhancer.

DISCUSSION

The experiments presented above used two different approaches to investigate the role of DNA binding by Runt in *slp1* regulation. The results provide compelling evidence that direct interactions between the Runt protein and *slp1 cis*-regulatory DNA contribute to the transcriptional regulation of this gene during *Drosophila* segmentation. The DNA-binding–defective Runt[CK] protein is compromised for both repression and activation of *slp1,* and mutagenesis of Runt-binding sites within the DESE enhancer affects both repression and activation mediated by this element in response to the Runt protein. Perhaps most interesting are the different contributions of DNA binding by Runt to DESE-dependent regulation depending on the presence or absence of the PESE enhancer, a distinct *cis*-regulatory element normally separated from DESE by more than 2.5 kb of DNA. When DESE is tested separately as an autonomous element, the Runt-binding sites are important for repression in type III cells where Runt and Ftz cooperate to repress *slp1* expression but have a small to no role in contributing to DESE-dependent activation in type II cells. However, when tested in a composite reporter gene construct that also includes the PESE enhancer, mutagenesis of the Runt-binding sites in DESE results in a significant reduction in the level of expression in type II cells.

One explanation for these observations is that a principal role of Runt's binding to DESE is to increase the strength of interaction between DESE and the *slp1* promoter, an activity that becomes most apparent when another enhancer, such as PESE, is competing for interaction with this promoter (Figure 7A). Given the context-dependent activities of the PESE and DESE enhancers, it is useful to consider this enhancer competition model in the context of the different *slp1* expression states (Figure 7, B and C). The initial description of nonadditive interactions between the wild-type DESE and PESE enhancers was based on the inappropriate expression driven by the DESE enhancer in type I cells anterior to the odd-numbered *slp1* stripes. This ectopic expression is suppressed in composite reporter gene constructs that also contain the PESE enhancer (Prazak *et al.*, 2010). As expected, mutagenesis of the Runt-binding sites in the DESE enhancer does not affect the inappropriate expression in type

expression in cells that do not express *slp1* (magenta cells anterior to stripes 6, 8, 10, and 12). (C) Quantitative expression pattern of *lacZ* confirms the accurate expression of the wild-type composite reporter with a decrease in intensity of the odd-numbered stripes. (D) Quantitative expression pattern of *lacZ* for the composite reporter with mutations in Runt-binding sites demonstrates the reduced expression of the odd-numbered stripes. The defect in repression of this reporter in type III cells by Runt and Ftz is revealed by the slight left-shifted shoulder to the peaks corresponding to the even-numbered stripes; this is most evident anterior to stripes 8 and 10. The integrated expression patterns in panels C and D were generated by averaging registered quantitative data obtained from seven and six stage 6 embryos, respectively. See Supplemental Figure 3 for the raw data black-and-white images of *slp1* and *lacZ* in situ hybridization of stage 6 embryos used for quantifying these expression patterns. (E) Statistical analysis of normalized expression data for the *slp[8765/3918]lacZ* (WT) and *slp[8765m1-5/3918]lacZ* (MT) reporters is provided with boxplots showing the range of expression along with a table of the mean expression values (both raw data and normalized) in different cell types from *slp1* stripes 3–12 along the A–P axis. Data points that were excluded as outliers are indicated by circles. As in Figure 5, the top row of the table indicates the location of the *slp1* stripes in relation to the boxplot above, and row 2 shows the four different cell types between *slp1* stripes 3 and 12. *LacZ* expression was measured as in Figure 5G at positions along the A–P axis established using the peaks of the averaged *slp1* mRNA expression patterns. The beige backgrounds identify boxplot data for type III cells. Table rows 3 and 4 report the averages of the measured *lacZ* expression levels for the different cell types in embryos with the WT and MT reporters, respectively. For more accurate comparison of *lacZ* expression levels, the same normalization method used in Figure 5 was applied to this data set. The normalized MT data (nMT) are provided in table row 5, and the ratio of the nMT to WT expression level in each cell type is shown in row 6. A Welch unpaired two-sample *t* test (one tailed) was conducted for each of the different cell types included in this figure. Significant differences in expression ($p < 0.05$) are highlighted in green (if $m_{WT} < m_{MT}$. m: mean of a group) to identify cells with an increase in *lacZ* expression in embryos containing the composite reporter with mutations in the Runt-binding sites. Conversely, significant differences in expression are highlighted in yellow ($m_{WT} > m_{MT}$) to identify cells for which the Runt-binding site mutations result in significantly reduced expression ($p < 0.05$).

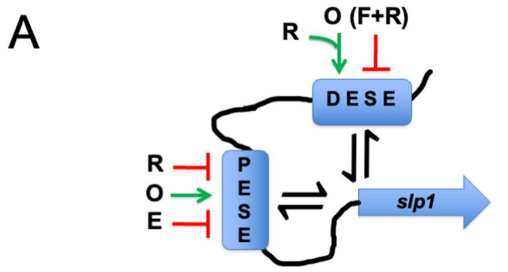

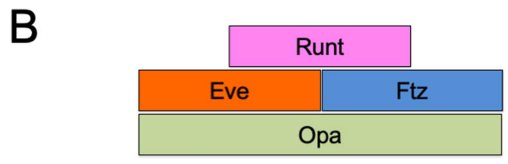

C

Cell-type	I	II	III	IV
$DESE^{WT}$	+ (0.48)	++ (1.01)	~ (0.13)	++
$DESE^{WT}$ + PESE	0	+ (0.30)	~ (0.08)	++
$DESE^{m1-5}$	+ (0.29)	++ (0.84)	++ (0.94)	++
$DESE^{m1-5}$ + PESE	0	~ (0.08)	+ (0.49)	++

FIGURE 7: Runt-dependent regulation of enhancer-promoter interactions. (A) Schematic diagram of the *slp1* locus. The DESE and PESE enhancers are depicted as blue boxes (labeled), and the blue arrow represents the *slp1* transcription unit. The ability of DESE to mediate activation by Opa (O) is indicated by a green arrow pointing toward DESE. The effect of Runt (R) in potentiating this Opa-dependent activation is indicated by the curved green line connected to this arrow. The requirement for both Runt and Ftz (R + F) in repressing DESE is indicated by the red line with a bar at the end. The ability of PESE to mediate activation by Opa as well as repression by either Runt or Eve (E) are indicated similarly to the left of the PESE enhancer. The proposed competitions of these two enhancers for interacting with the *slp1* promoter are represented by bidirectional black arrows between each enhancer and the promoter region. The expression of *slp1* produced by these different regulatory inputs is diagramed below in B, which shows the relative phasing of Runt, Eve, Ftz, and Opa expression above a column of eight cells, corresponding to one odd and one even parasegment (PS). Cells that express *slp1* are shaded green, with the darker shading representing the stronger early expression in the even-numbered parasegments. The PESE enhancer can mediate the Eve-dependent repression of *slp1* in type I cells (Prazak *et al.*, 2010). Runt prevents PESE-dependent expression in both type II and type III cells. The DESE-dependent expression of the odd-numbered *slp1* stripes in type II cells requires both Runt and Opa, whereas this same enhancer mediates repression in response to the combination of both Runt and Ftz in type III cells. Both enhancers are capable of driving expression in type IV cells. (C) Table indicating the relative expression level in type I, II, and III cells relative to the high expression levels in type IV cells for DESE-containing reporter genes with the wild-type ($DESE^{WT}$) or Runt-binding site mutant ($DESE^{m1-5}$) enhancer, either alone or in a composite reporter also containing the PESE enhancer. A high average expression at a level 80% or higher of that in the type IV cells is indicated as ++. Intermediate expression levels, 25–50% of that in type IV cells, are indicated with a +. An average that is above background but less than 15% of that in type IV cells is indicated with a ~. These numbers were generated by calculating the expression for each of the different type I, II, and III cells relative to the type IV cell used for normalizing expression values in Figures 5G and 6E and then averaging these values for the four different type I cells and five different type II and III cells included in these figures.

I cells (Figure 5G), as Runt is not normally expressed in these cells (Figure 7B). PESE also interferes with the ectopic expression driven by the mutant DESE enhancer in cell type I (Figures 6, A′, B′, and E, and 7C). Taken altogether these observations suggest that PESE, which normally mediates repression in cell type I interferes with Runt-independent, DESE-driven expression in this cell type.

Further evidence in support of the repressive effect of PESE on DESE activity comes from considering the expression of these different reporter genes in cell type II. Expression of the odd-numbered *slp1* stripes in cell type II requires both Runt and Opa and is mediated by the DESE enhancer (Prazak *et al.*, 2010). When tested as an autonomous element, the wild-type DESE enhancer drives abnormally high levels of reporter gene expression in type II cells that are comparable to the levels observed in type IV cells (Figures 2G and 5, D and G). Inclusion of PESE in the composite reporter containing the DESE enhancer reduces expression in type II cells, giving a difference in the expression levels in these two cell types similar to that observed for *slp1* (Figures 2A″ and 6A″). Mutagenesis of the Runt-binding sites in DESE in a composite reporter containing the PESE enhancer results in significantly reduced expression in type II cells (Figures 6 and 7C). In the context of the enhancer competition model, these observations suggest that Runt binding to DESE increases the ability to overcome the repressive effects of PESE in type II cells by augmenting interactions between DESE and the *slp1* promoter.

The above discussion identifies the repressive effects of PESE on DESE-dependent expression in cell types I and II (Figure 7C). Prior work provides additional evidence that PESE is also capable of interfering with DESE-dependent expression in cell type IV. Like cell type I, Runt is not expressed in cell type IV, and this aspect of DESE-driven expression should be Runt independent. When tested as an autonomous enhancer, DESE drives expression in the type IV cells that normally comprise the even-numbered *slp1* stripes, and this expression is insensitive to repression by Eve (Prazak *et al.*, 2010). Ectopic Eve specifically represses the even-numbered stripes of both *slp1* and composite reporter gene constructs containing both the PESE and DESE enhancers. Our interpretation is that ectopic Eve blocks DESE-dependent expression in these cells by repressing PESE in a manner that does not allow for DESE-driven expression. The Eve-dependent repression of PESE involves preventing release of promoter-proximal paused RNA polymerase. It has been proposed that repression at this step involves a stable association of PESE with the *slp1* promoter that occludes access to the DESE enhancer (Hang and Gergen, 2017). The same explanation could also apply to the effects of PESE on DESE-dependent expression observed in cell types I and II.

We further suggest that a competition between the PESE and DESE enhancers can account for the temporal dynamics of *slp1* expression. Expression of the even-numbered *slp1* stripes in cell type IV is strong in early cellular blastoderm stage embryos, whereas

expression of the odd-numbered stripes in type II cells emerges later. Both PESE and DESE drive strong expression in type IV cells. The autonomous DESE enhancer can also drive strong expression in type II cells, but not when in competition with the PESE. The four-cell-wide pair-rule stripes of Eve shrink during the cellular blastoderm stage as expression is progressively lost from the more posterior cells in these stripes (Clark and Akam, 2016). We propose that the repression of PESE in cell type II is relaxed as Eve expression levels drop, thus allowing the DESE enhancer to access the *slp1* promoter. The differences in expression of the wild-type and Runt-binding site mutant DESE enhancer in cell type II when these enhancers are confronted with competition from PESE indicate a role for DNA binding by Runt in promoting DESE activity during the dynamic regulatory interplay between these two enhancers.

Other examples of nonadditive interactions between distinct enhancers, in both *Drosophila* and mouse and human cells, have been interpreted to be due to competitive interactions between these enhancers and the promoter (Lin *et al.*, 2007; Perry *et al.*, 2010; Bhattacharyya *et al.*, 2011; Dib *et al.*, 2011; Dunipace *et al.*, 2011; Bothma *et al.*, 2015; El-Sherif and Levine, 2016; Waymack *et al.*, 2020). Much of this work has focused on so-called shadow enhancers with largely overlapping expression patterns that are interpreted to buffer expression levels against changes in temperature or to suppress noise. The competitive repressive effect of PESE on DESE-dependent transcription that we describe is most similar to the dominant repressive effects that have been characterized for enhancer pairs from the *Drosophila* gap genes *Kr* and *kni* that contribute to dynamic shifts in the borders of expression (El-Sherif and Levine, 2016).

An important implication of these findings is that *cis*-regulatory elements that normally contribute to specific aspects of an expression pattern may have broader activities as autonomous elements, even when tested in a physiologically relevant cellular context. A survey of prospective enhancers from genes expressed in the *Drosophila* brain reveals that these elements frequently drive expression in cells that normally do not express the endogenous gene (Pfeiffer *et al.*, 2008). This observation parallels our observations on the *slp1* DESE enhancer and strongly suggests that nonautonomous regulation of enhancer activity is a phenomenon of widespread importance. Our knowledge on the set of transcription factors that are responsible for the nonadditive interactions between the two *slp1* enhancers, coupled with the tools available for studies in the *Drosophila* embryo, provides an exceptional platform for further investigating the molecular basis of these regulatory phenomena.

MATERIALS AND METHODS

Request a protocol through *Bio-protocol*.

Construction of *slp1-lacZ* reporters

The composite P-element reporter gene construct *slp1[8765:3918]lacZ*^{P} obtained by standard P-element germline transformation and the *slp1[3918]lacZ*^{att} and *slp1[8771]lacZ*^{att} transgenes integrated into the same chromosomal using site ΦC31-mediated recombination are as described (Prazak *et al.*, 2010). The original *slp1[3918]lacZ*^{att} and *slp[8771]lacZ*^{att} transgenes and the Runx-binding site mutant derivatives of this reporter gene contain *slp1* basal promoter sequences from base pairs –72 to +57. The Runx binding site mutants were generated by first cloning a *slp1* –8.7 kb to –6.5 kb *Xba*I/*Not*I fragment from pC:*slp1[8765]lacZ*^{P} (Prazak *et al.*, 2010) into the corresponding sites of pBluescript to generate pB:slp1[8765]. This construct was then used for PCR using complementary primers (sequence available upon request) that change the two critical cytosines in the consensus sequence to adenine resulting in two fragments that extend to the flanking *M13* forward and reverse primers. These fragments were mixed and amplified with *M13* forward and reverse primers and cloned into the *Xba*I and *Not*I sites of pBluescript creating pB:slp[8765m2], pBslp[8765m4], pBslp[8765m5], pB:slp1[8765m3,4], and pB:slp1[8765m1,2,3,4,5]. After confirming the sequence, primers that amplify from 8710 to 7136 base pairs upstream of *slp1* were used to amplify DNA segments containing the binding site mutations such that these DNA segments could be cloned into the *Xho*I site of pC:*slp1*^{BP}*-lacZ*^{att} using the In-Fusion Dry-Down PCR Cloning Kit (Clontech) to generate pC:*slp1[8771m2]lacZ*^{att}, pC:*slp1[8771m4]lacZ*^{att}, pC:*slp1[8771m5]lacZ*^{att}, pC:*slp1[8771m3,4]lacZ*^{att}, and pC:*slp1[8771-5]lacZ*^{att}.

The original *slp1[8765:3918]lacZ*^{P} composite reporter construct contains *slp1* basal promoter sequences spanning from –260 to +121. To generate similar composite reporter gene constructs for integration using ΦC31 transgenesis, this extended basal promoter was obtained by PCR amplification from genomic subclones with the addition of upstream *Xho*I and downstream *Kpn*I sites and cloned into pBluescript to create pB:*slp1[LBP]*. This basal promoter segment was moved into pC:*slp1-link-lacZ*^{att} w, where a linker was introduced to replace Bluescript polylinker between the *Eco*RI and *Xho*I sites upstream of the basal promoter with unique *Not*I, *Sph*I, *Stu*I, and *Spe*I sites as an *Eco*RI + *Kpn*I fragment removing the smaller basal promoter and creating pC:*slp1*^{LBP}*-link -lacZ*^{att}. This vector was digested with *Eco*RI treated with Klenow, then digested with *Not*I, and then ligated to a gel-purified DESE-containing segment of either pB:slp1[8765] or pB:slp[8765m1,2,3,4,5] that had been digested with *Xba*I treated with Klenow and digested with *Not*I to generate pC:*slp1[8765]lacZ*^{att} and pC:*slp1[8765m1-5]lacZ*^{att}, respectively. The composite *slp1[8765:3918]lacZ*^{att} and *slp1[8765m1-5:3918]lacZ*^{att} constructs were obtained by inserting the PESE-containing *Not*I fragment from pB:*slp1*[1839] into the *Not*I site of the corresponding parental pC:*slp1[8765]lacZ*^{att} plasmid.

ΦC31-mediated transgenic lines were obtained using the *attP* integration site on the third chromosome (Groth *et al.*, 2004). Constructs containing the *attB* sequence were coinjected with ΦC31 mRNA into *y w; P{CaryP}attP2* embryos, the surviving adult progeny backcrossed to the parental line, and the F1 generation screened for *white*$^{+}$transformants. ΦC31 mRNA was generated from *Bam*HI linearized pET-phiC31-polyA template with the mMessage mMachine high yield Capped RNA Transcription Kit (Ambion), and mRNA was recovered via LiCl precipitation without DNase treatment.

Drosophila mutants and genetics

Ectopic expression of pair-rule transcription factors was achieved using the *NGT* maternal expression system. The second chromosome linked *P{GAL4-nos.NGT}40* (*NGT40*) driver and the *P{UAS-runt.T}15, P{UAS-runt.T}232, P{UAS-runt[CK]}43*, *P{UAS-runt[CK]}77*, *P{UAS-opa.VZ}D10*, and *P{UAS-opa.VZ}14* transgenes have been described previously (Tracey *et al.*, 2000; Vander Zwan *et al.*, 2003; Swantek and Gergen, 2004). The *P{UAS-ftz}263* and *P{UAS-eve}12* transgenes were provided to us by Leslie Pick (Lohr and Pick, 2005) and John Reinitz (Zallen and Wieschaus, 2004), respectively. Embryos were collected from crosses between females homozygous for *NGT40* and for the different third chromosome–linked reporter genes and males carrying these different *UAS* transgenes.

Whole-mount in situ hybridization

Embryos were collected as described (Tsai and Gergen, 1994). Fluorescence in situ hybridization was carried out as described (Janssens *et al.*, 2005) with the following modification: After fixation embryos

were cleared in xylenes:ethanol (9:1) and then postfixed in Phosphate buffered saline with 0.1% (v/v) Tween 20 (PBT) + 5% formaldehyde. Embryos were permeabilized for 10 min in 80% acetone in H_2O at –20°C. The fluorescein-labeled *lacZ* riboprobe was synthesized with fluorescein-12-UTP (Roche) in place of digoxigenin-conjugated UTP (Tsai and Gergen, 1994). After hybridization, *lacZ* mRNA was visualized by sequential incubation with rabbit anti-fluorescein (1 µg/ml final) and Alexa Fluor 647 donkey anti-rabbit (1 µg/ml) antibodies (Molecular Probes). The digoxigenin-labeled riboprobe for *slp1* is as described in Wheeler *et al.* (2002). Digoxigenin-labeled probes were detected using mouse anti-digoxigenin antibody (Roche; 1.25 µg/ml final) followed by Alexa Fluor 555 goat anti-mouse (1 µg/ml) and Alexa Fluor 555 donkey anti-goat (1 µg/ml) antibodies (Molecular Probes). Blocking was done in 2× Western Blocking Reagent (Roche) diluted in PBT. All antibodies were preabsorbed at a 10× concentration in PBT with 1/10 volume of 0–12 h embryos and then diluted to 1×. PicoGreen (Molecular Probes) was used to stain nuclei at a 1:30,000 dilution. Before mounting, embryos were washed in phosphate-buffered saline:glycerol (1:1) for 20 min and then mounted in 45 µl mounting medium (2.5% Dabco [Sigma], 50 mM Tris [pH 8.0], and 90% glycerol) and covered with a Corning 22 × 40-mm cover glass (No. 1 ½). Images were obtained on a Leica TCS SP2 Spectral Confocal Microscope system as described (Janssens *et al.*, 2005).

Electrophoretic mobility shift assay (EMSA)

EMSA experiments to detect DNA binding of Runt:Bro protein complexes were done as described by Kramer *et al.* (1999) with a 37 base pair radiolabeled DNA probe containing the Runx site in the A-element of the polyoma virus enhancer. Pure competitor oligonucleotides containing Runx sites of different affinities (Lewis *et al.*, 1999) were obtained from Nancy Speck (University of Pennsylvania).

ChIP analysis

The ChIP assays were performed as described previously (Wang *et al.*, 2007) using chromatin prepared from 3- to 4-h embryo collections with either a rabbit anti-Runt antibody or normal rabbit serum from Sigma. The primer sequences used in quantitative PCR (qPCR) are available upon request. (Error bars represent the mean SE from three independent immunoprecipitation experiments.)

Sequencing results

Input as well as Runt immunoprecipitated DNA were sequenced by the Stony Brook Sequencing Facility using primers specific to a region of DESE that contains Runt site 4 (Figure 4C) and that will amplify this region from both endogenous *slp1* as well the DESE-containing reporter gene.

Quantification of expression patterns

Laterally oriented embryos were scanned using a Leica TCS SP2 Spectral Confocal Microscope System as in Janssens *et al.* (2005) with quantification of the expression of different reporters performed essentially as described by Surkova *et al.* (2008a,b). Pico Green (Molecular Probes) was used to detect nuclei as well as to find the correct focal plane. To compare the expression levels in different embryos, the same microscope gain and offset were used for each image scan. These settings were adjusted to just below saturation on stage 7 embryos that have stronger *slp1* expression than the stage 6 embryos used for quantification. Each microscope channel was scanned sequentially 16 times in each of two focal planes. Scans for each plane were averaged to reduce noise. The set of images for one embryo were segmented by creating a nuclear mask using nuclear marker image software. Quantitative expression data were stored in a tabular ASCII file containing one line per segmented nucleus. Each nucleus was characterized by a unique identification number, the *x* and *y* coordinates of its centroid and the average fluorescence levels of the *slp1* and *lacZ* mRNAs. The *x*- and *y*-axis coordinates, corresponding to the position on the A–P and D–V axes, are expressed as percent of the embryo length and width, respectively. Background staining in the microscopic images was removed before further image analysis (Myasnikova *et al.*, 2005). The background level in each pattern was approximated by quadratic paraboloid, the parameters of which were determined by fitting to the data in nonexpressing areas. To facilitate better approximation results the data were smoothed with low-pass filter of wavelet transform. Stage 6 embryos were identified based on their distinctive differential interference contrast morphology and *slp1* mRNA pattern. Integrated data that average the patterns of individual embryos were generated to eliminate variability from individual embryos. To do this, the *slp1* expression pattern was used to register the different embryos. Registration was performed by affine transformation of the nuclear coordinates along the A–P axis so that the ground control points (GCPs) in all patterns coincide as closely as possible (Myasnikova *et al.*, 2001). The extrema of the 1D *slp1* expression pattern were used as GCPs for registration. This set consisted of 23 points and did not include stripes 0 and 1. The GCPs were extracted using fast dyadic wavelet transform and the integrated data produced by averaging the registered individual patterns (Kozlov *et al.*, 2009).

ACKNOWLEDGMENTS

The technical contributions of Sohail Anwar and Yelena Alshuller, the *Drosophila* stocks provided by Leslie Pick and John Reinitz, the purified Runx-site containing oligonucleotides provided by Nancy Speck and the anti-Runt antisera provided by Eric Wieschaus are all greatly appreciated. The manuscript benefited from inputs by Howard Sirotkin, Deniz Erezyilmaz, Kimberly Bell, and Saiyu Hang. This research was supported by Award Number MCB 0721430 from the National Science Foundation (NSF) and Award Number R01GM094401 from the National Institute of General Medical Sciences (NIGMS). The content is solely the responsibility of the authors and does not necessarily represent the official views of the NSF, the NIGMS, or the National Institutes of Health. This article is dedicated to the memory of Kevin King.

REFERENCES

Akech J, Wixted JJ, Bedard K, van der Deen M, Hussain S, Guise TA, van Wijnen AJ, Stein JL, Languino LR, Altieri DC, *et al.* (2010). Runx2 association with progression of prostate cancer in patients: mechanisms mediating bone osteolysis and osteoblastic metastatic lesions. Oncogene 29, 811–821.

Bhattacharyya S, Tian J, Bouhassira EE, Locker J (2011). Systematic targeted integration to study *albumin* gene control elements. PLoS One 6, e23234.

Bothma JP, Garcia HG, Ng S, Perry MW, Gregor T, Levine M (2015). Enhancer additivity and non-additivity are determined by enhancer strength in the Drosophila embryo. eLife 4, e07956.

Bravo J, Li Z, Speck NA, Warren AJ (2001). The leukemia-associated AML1 (Runx1)–CBF beta complex functions as a DNA-induced molecular clamp. Nat Struct Biol 8, 371–378.

Cao S, Wang C, Zheng Q, Qiao Y, Xu K, Jiang T, Wu A (2011). STAT5 regulates glioma cell invasion by pathways dependent and independent of STAT5 DNA binding. Neurosci Lett 487, 228–233.

Cheung E, Acevedo ML, Cole PA, Kraus WL (2005). Altered pharmacology and distinct coactivator usage for estrogen receptor-dependent transcription through activating protein-1. Proc Natl Acad Sci USA 102, 559–564.

Clark E, Akam M (2016). Odd-paired controls frequency doubling in Drosophila segmentation by altering the pair-rule gene regulatory network. eLife 5, e18215.
de Bruijn MF, Speck NA (2004). Core-binding factors in hematopoiesis and immune function. Oncogene 23, 4238–4248.
Delerive P, De Bosscher K, Vanden Berghe W, Fruchart JC, Haegeman G, Staels B (2002). DNA binding-independent induction of IkappaBalpha gene transcription by PPARalpha. Mol Endocrinol 16, 1029–1039.
Dib S, Denarier E, Dionne N, Beaudoin M, Friedman HH, Peterson AC (2011). Regulatory modules function in a non-autonomous manner to control transcription of the mbp gene. Nucleic Acids Res 39, 2548–2558.
Duffy JB, Gergen JP (1994). Sex, segments, and the central nervous system: common genetic mechanisms of cell fate determination. Adv Genet 31, 1–28.
Dunipace L, Ozdemir A, Stathopoulos A (2011). Complex interactions between cis-regulatory modules in native conformation are critical for Drosophila snail expression. Development 138, 4075–4084.
El-Sherif E, Levine M (2016). Shadow enhancers mediate dynamic shifts of gap gene expression in the Drosophila embryo. Curr Biol 26, 1164–1169.
Enomoto H, Furuichi T, Zanma A, Yamana K, Yoshida C, Sumitani S, Yamamoto H, Enomoto-Iwamoto M, Iwamoto M, Komori T (2004). Runx2 deficiency in chondrocytes causes adipogenic changes in vitro. J Cell Sci 117, 417–425.
Gamou T, Kitamura E, Hosoda F, Shimizu K, Shinohara K, Hayashi Y, Nagase T, Yokoyama Y, Ohki M (1998). The partner gene of AML1 in t(16;21) myeloid malignancies is a novel member of the MTG8(ETO) family. Blood 91, 4028–4037.
Gergen JP, Wieschaus E (1986). Dosage requirements for runt in the segmentation of Drosophila embryos. Cell 45, 289–299.
Gergen JP, Wieschaus EF (1985). The localized requirements for a gene affecting segmentation in Drosophila: analysis of larvae mosaic for runt. Dev Biol 109, 321–335.
Goel A, Arnold CN, Tassone P, Chang DK, Niedzwiecki D, Dowell JM, Wasserman L, Compton C, Mayer RJ, Bertagnolli MM, Boland CR (2004). Epigenetic inactivation of RUNX3 in microsatellite unstable sporadic colon cancers. Int J Cancer 112, 754–759.
Golub TR, Barker GF, Bohlander SK, Hiebert SW, Ward DC, Bray-Ward P, Morgan E, Raimondi SC, Rowley JD, Gilliland DG (1995). Fusion of the TEL gene on 12p13 to the AML1 gene on 21q22 in acute lymphoblastic leukemia. Proc Natl Acad Sci USA 92, 4917–4921.
Groth AC, Fish M, Nusse R, Calos MP (2004). Construction of transgenic Drosophila by using the site-specific integrase from phage phiC31. Genetics 166, 1775–1782.
Hang S, Gergen JP (2017). Different modes of enhancer-specific regulation by Runt and Even-skipped during Drosophila segmentation. Mol Biol Cell 28, 681–691.
Helms C, Cao L, Krueger JG, Wijsman EM, Chamian F, Gordon D, Heffernan M, Daw JA, Robarge J, Ott J, *et al*. (2003). A putative RUNX1 binding site variant between SLC9A3R1 and NAT9 is associated with susceptibility to psoriasis. Nat Genet 35, 349–356.
Ito Y (2004). Oncogenic potential of the RUNX gene family: "overview." Oncogene 23, 4198–4208.
Janssens H, Kosman D, Vanario-Alonso CE, Jaeger J, Samsonova M, Reinitz J (2005). A high-throughput method for quantifying gene expression data from early Drosophila embryos. Dev Genes Evol 215, 374–381.
Kagoshima H, Shigesada K, Satake M, Ito Y, Miyoshi H, Ohki M, Pepling M, Gergen P (1993). The Runt domain identifies a new family of heteromeric transcriptional regulators. Trends Genet 9, 338–341.
Kamachi Y, Ogawa E, Asano M, Ishida S, Murakami Y, Satake M, Ito Y, Shigesada K (1990). Purification of a mouse nuclear factor that binds to both the A and B cores of the polyomavirus enhancer. J Virol 64, 4808–4819.
Kayed H, Jiang X, Keleg S, Jesnowski R, Giese T, Berger MR, Esposito I, Lohr M, Friess H, Kleeff J (2007). Regulation and functional role of the Runt-related transcription factor-2 in pancreatic cancer. Br J Cancer 97, 1106–1115.
Kitago M, Martinez SR, Nakamura T, Sim MS, Hoon DS (2009). Regulation of RUNX3 tumor suppressor gene expression in cutaneous melanoma. Clin Cancer Res 15, 2988–2994.
Kozlov KN, Myasnikova E, Samsonova AA, Surkova S, Reinitz J, Samsonova M (2009). GCPReg package for registration of the segmentation gene expression data in Drosophila. Fly (Austin) 3, 151–156.
Kramer SG, Jinks TM, Schedl P, Gergen JP (1999). Direct activation of Sex-lethal transcription by the Drosophila runt protein. Development 126, 191–200.
Lau QC, Raja E, Salto-Tellez M, Liu Q, Ito K, Inoue M, Putti TC, Loh M, Ko TK, Huang C, *et al*. (2006). RUNX3 is frequently inactivated by dual mechanisms of protein mislocalization and promoter hypermethylation in breast cancer. Cancer Res 66, 6512–6520.
Lewis AF, Stacy T, Green WR, Taddesse-Heath L, Hartley JW, Speck NA (1999). Core-binding factor influences the disease specificity of Moloney murine leukemia virus. J Virol 73, 5535–5547.
Li LH, Gergen JP (1999). Differential interactions between Brother proteins and Runt domain proteins in the Drosophila embryo and eye. Development 126, 3313–3322.
Lian JB, Balint E, Javed A, Drissi H, Vitti R, Quinlan EJ, Zhang L, Van Wijnen AJ, Stein JL, Speck N, Stein GS (2003). Runx1/AML1 hematopoietic transcription factor contributes to skeletal development in vivo. J Cell Physiol 196, 301–311.
Lin Q, Chen Q, Lin L, Smith S, Zhou J (2007). Promoter targeting sequence mediates enhancer interference in the Drosophila embryo. Proc Natl Acad Sci USA 104, 3237–3242.
Liu N, Barbosa AC, Chapman SL, Bezprozvannaya S, Qi X, Richardson JA, Yanagisawa H, Olson EN (2009). DNA binding-dependent and -independent functions of the Hand2 transcription factor during mouse embryogenesis. Development 136, 933–942.
Lohr U, Pick L (2005). Cofactor-interaction motifs and the cooption of a homeotic Hox protein into the segmentation pathway of Drosophila melanogaster. Curr Biol 15, 643–649.
MacArthur S, Li XY, Li J, Brown JB, Chu HC, Zeng L, Grondona BP, Hechmer A, Simirenko L, Keranen SV, *et al*. (2009). Developmental roles of 21 Drosophila transcription factors are determined by quantitative differences in binding to an overlapping set of thousands of genomic regions. Genome Biol 10, R80.
Melnikova IN, Crute BE, Wang S, Speck NA (1993). Sequence specificity of the core-binding factor. J Virol 67, 2408–2411.
Miyoshi H, Kozu T, Shimizu K, Enomoto K, Maseki N, Kaneko Y, Kamada N, Ohki M (1993). The t(8;21) translocation in acute myeloid leukemia results in production of an AML1-MTG8 fusion transcript. EMBO J 12, 2715–2721.
Mizugishi K, Aruga J, Nakata K, Mikoshiba K (2001). Molecular properties of Zic proteins as transcriptional regulators and their relationship to GLI proteins. J Biol Chem 276, 2180–2188.
Mundlos S, Otto F, Mundlos C, Mulliken JB, Aylsworth AS, Albright S, Lindhout D, Cole WG, Henn W, Knoll JH, *et al*. (1997). Mutations involving the transcription factor CBFA1 cause cleidocranial dysplasia. Cell 89, 773–779.
Myasnikova E, Samsonova A, Kozlov K, Samsonova M, Reinitz J (2001). Registration of the expression patterns of Drosophila segmentation genes by two independent methods. Bioinformatics 17, 3–12.
Myasnikova E, Samsonova M, Kosman D, Reinitz J (2005). Removal of background signal from in situ data on the expression of segmentation genes in Drosophila. Dev Genes Evol 215, 320–326.
Nucifora G, Begy CR, Erickson P, Drabkin HA, Rowley JD (1993). The 3;21 translocation in myelodysplasia results in a fusion transcript between the AML1 gene and the gene for EAP, a highly conserved protein associated with the Epstein-Barr virus small RNA EBER 1. Proc Natl Acad Sci USA 90, 7784–7788.
Nusslein-Volhard C, Wieschaus E (1980). Mutations affecting segment number and polarity in Drosophila. Nature 287, 795–801.
Otto F, Thornell AP, Crompton T, Denzel A, Gilmour KC, Rosewell IR, Stamp GW, Beddington RS, Mundlos S, Olsen BR, *et al*. (1997). Cbfa1, a candidate gene for cleidocranial dysplasia syndrome, is essential for osteoblast differentiation and bone development. Cell 89, 765–771.
Perry MW, Boettiger AN, Bothma JP, Levine M (2010). Shadow enhancers foster robustness of Drosophila gastrulation. Curr Biol 20, 1562–1567.
Pfeiffer BD, Jenett A, Hammonds AS, Ngo TT, Misra S, Murphy C, Scully A, Carlson JW, Wan KH, Laverty TR, *et al*. (2008). Tools for neuroanatomy and neurogenetics in Drosophila. Proc Natl Acad Sci USA 105, 9715–9720.
Porter W, Saville B, Hoivik D, Safe S (1997). Functional synergy between the transcription factor Sp1 and the estrogen receptor. Mol Endocrinol 11, 1569–1580.
Pratap J, Wixted JJ, Gaur T, Zaidi SK, Dobson J, Gokul KD, Hussain S, van Wijnen AJ, Stein JL, Stein GS, Lian JB (2008). Runx2 transcriptional activation of Indian Hedgehog and a downstream bone metastatic pathway in breast cancer cells. Cancer Res 68, 7795–7802.
Prazak L, Fujioka M, Gergen JP (2010). Non-additive interactions involving two distinct elements mediate sloppy-paired regulation by pair-rule transcription factors. Dev Biol 344, 1048–1059.

Prokunina L, Castillejo-Lopez C, Oberg F, Gunnarsson I, Berg L, Magnusson V, Brookes AJ, Tentler D, Kristjansdottir H, Grondal G, *et al.* (2002). A regulatory polymorphism in PDCD1 is associated with susceptibility to systemic lupus erythematosus in humans. Nat Genet 32, 666–669.

Ravet E, Reynaud D, Titeux M, Izac B, Fichelson S, Romeo PH, Dubart-Kupperschmitt A, Pflumio F (2004). Characterization of DNA-binding-dependent and -independent functions of SCL/TAL1 during human erythropoiesis. Blood 103, 3326–3335.

Reichardt HM, Kaestner KH, Tuckermann J, Kretz O, Wessely O, Bock R, Gass P, Schmid W, Herrlich P, Angel P, Schutz G (1998). DNA binding of the glucocorticoid receptor is not essential for survival. Cell 93, 531–541.

Shin EJ, Kim HJ, Son MW, Ahn TS, Lee HY, Lim DR, Bae SB, Jeon S, Kim H, Jeong D, *et al.* (2018). Epigenetic inactivation of RUNX3 in colorectal cancer. Ann Surg Treat Res 94, 19–25.

Sullivan JC, Sher D, Eisenstein M, Shigesada K, Reitzel AM, Marlow H, Levanon D, Groner Y, Finnerty JR, Gat U (2008). The evolutionary origin of the Runx/CBFbeta transcription factors–studies of the most basal metazoans. BMC Evol Biol 8, 228.

Surkova S, Myasnikova E, Janssens H, Kozlov KN, Samsonova AA, Reinitz J, Samsonova M (2008a). Pipeline for acquisition of quantitative data on segmentation gene expression from confocal images. Fly (Austin) 2, 58–66.

Surkova SY, Myasnikova EM, Kozlov KN, Samsonova AA, Reinitz J, Samsonova MG (2008b). Methods for acquisition of quantitative data from confocal images of gene expression in situ. Cell Tissue Biol 2, 200–215.

Swantek D, Gergen JP (2004). Ftz modulates Runt-dependent activation and repression of segment-polarity gene transcription. Development 131, 2281–2290.

Tahirov TH, Inoue-Bungo T, Morii H, Fujikawa A, Sasaki M, Kimura K, Shiina M, Sato K, Kumasaka T, Yamamoto M, *et al.* (2001). Structural analyses of DNA recognition by the AML1/Runx-1 Runt domain and its allosteric control by CBFbeta. Cell 104, 755–767.

Tang YY, Crute BE, Kelley JJ, Huang X, Yan J, Shi J, Hartman KL, Laue TM, Speck NA, Bushweller JH (2000). Biophysical characterization of interactions between the core binding factor alpha and beta subunits and DNA. FEBS Lett 470, 167–172.

Tokuhiro S, Yamada R, Chang X, Suzuki A, Kochi Y, Sawada T, Suzuki M, Nagasaki M, Ohtsuki M, Ono M, *et al.* (2003). An intronic SNP in a RUNX1 binding site of SLC22A4, encoding an organic cation transporter, is associated with rheumatoid arthritis. Nat Genet 35, 341–348.

Tracey WD Jr, Ning X, Klingler M, Kramer SG, Gergen JP (2000). Quantitative analysis of gene function in the Drosophila embryo. Genetics 154, 273–284.

Tsai C, Gergen JP (1994). Gap gene properties of the pair-rule gene runt during Drosophila segmentation. Development 120, 1671–1683.

Tuckermann JP, Reichardt HM, Arribas R, Richter KH, Schutz G, Angel P (1999). The DNA binding-independent function of the glucocorticoid receptor mediates repression of AP-1-dependent genes in skin. J Cell Biol 147, 1365–1370.

Umayahara Y, Kawamori R, Watada H, Imano E, Iwama N, Morishima T, Yamasaki Y, Kajimoto Y, Kamada T (1994). Estrogen regulation of the insulin-like growth factor I gene transcription involves an AP-1 enhancer. J Biol Chem 269, 16433–16442.

Vander Zwan CJ, Wheeler JC, Li LH, Tracey WD, Gergen JP (2003). A DNA-binding-independent pathway of repression by the Drosophila Runt protein. Blood Cells Mol Dis 30, 207–222.

Walrad PB, Hang S, Joseph GS, Salas J, Gergen JP (2010). Distinct contributions of conserved modules to runt transcription factor activity. Mol Biol Cell 21, 2315–2326.

Wang X, Lee C, Gilmour DS, Gergen JP (2007). Transcription elongation controls cell fate specification in the Drosophila embryo. Genes Dev 21, 1031–1036.

Waymack R, Fletcher A, Enciso G, Wunderlich Z (2020). Shadow enhancers can suppress input transcription factor noise through distinct regulatory logic. eLife 9, e59351.

Weersma RK, Zhou L, Nolte IM, van der Steege G, van Dullemen HM, Oosterom E, Bok L, Peppelenbosch MP, Faber KN, Kleibeuker JH, Dijkstra G (2008). Runt-related transcription factor 3 is associated with ulcerative colitis and shows epistasis with solute carrier family 22, members 4 and 5. Inflamm Bowel Dis 14, 1615–1622.

Wheeler JC, VanderZwan C, Xu X, Swantek D, Tracey WD, Gergen JP (2002). Distinct in vivo requirements for establishment versus maintenance of transcriptional repression. Nat Genet 32, 206–210.

Wildey GM, Howe PH (2009). Runx1 is a co-activator with FOXO3 to mediate transforming growth factor beta (TGFbeta)-induced Bim transcription in hepatic cells. J Biol Chem 284, 20227–20239.

Yamagata T, Maki K, Mitani K (2005). Runx1/AML1 in normal and abnormal hematopoiesis. Int J Hematol 82, 1–8.

Zallen JA, Wieschaus E (2004). Patterned gene expression directs bipolar planar polarity in Drosophila. Dev Cell 6, 343–355.

Zhang L, Li Z, Yan J, Pradhan P, Corpora T, Cheney MD, Bravo J, Warren AJ, Bushweller JH, Speck NA (2003). Mutagenesis of the Runt domain defines two energetic hot spots for heterodimerization with the core binding factor beta subunit. J Biol Chem 278, 33097–33104.

Zhang Z, Chen G, Cheng Y, Martinka M, Li G (2011). Prognostic significance of RUNX3 expression in human melanoma. Cancer 117, 2719–2727.